



Evaluating anti-inflammatory and anti-oxidative potentialities of the chloroform fraction of *Asparagus racemosus* roots against cisplatin induced acute kidney injury

Sahadeb Jana^{a,b}, Palash Mitra^{a,b}, Titli Panchali^{a,b}, Amina Khatun^{a,b}, Tridip Kumar Das^{a,b}, Kuntal Ghosh^b, Shrabani Pradhan^b, Sudipta Chakrabarti^b, Suchismita Roy^{b,*}

^a Biodiversity and Environmental Studies Research Centre affiliated to Vidyasagar University, Midnapore City College, Bhadutala, Paschim Medinipur, 721129, West Bengal, India

^b Department of Paramedical and Allied Health Sciences, Midnapore City College, Kuturiya, Bhadutala, Midnapore, 721129, India

ARTICLE INFO

Handling Editor: Dr. P Fernandes

Keywords:

Acute kidney injury
Oxidative stress
Inflammation
Asparagus racemosus
Phytomolecules

ABSTRACT

Ethnopharmacological relevance: Acute kidney injury (AKI), a global public health concern that increases the risk of death, end-stage renal disease, and prolonged hospital admissions. As of this point, supportive measures like fluid resuscitation and replacement therapy for renal failure are the only treatments available for treating AKI. *Asparagus racemosus* (AR) also known as Shatavari, belongs to family Liliaceae and is considered exceptional in Ayurvedic medicine due to its versatility in treating and preventing a variety of illnesses.

Aim of the study: The purpose of this study is to determine the effectiveness of chloroform fraction of *Asparagus racemosus* (CFAR) against cisplatin (CP) induced AKI.

Materials and methods: HPLC was used to analyze the presence of bioactive phytochemicals in CFAR using standard quercetin. Further LC-MS study indicated the existence of different bioactive compounds. Normal Rat Kidney (NRK-52E) cells were used to study the nephroprotective effect of CFAR. Cells were untreated, treated or cotreated with CP (20 μ M) and CFAR (5, 25, 50, 100, 200 and 400 μ g/mL) for 24 h. After 24 h of treatment, cell viability assay and assay of apoptosis parameters were performed. The CFAR at the dose of 50 mg, 100 mg and 200 mg/kg/day was administered orally for 15 days and acute kidney injury was induced in rats by intraperitoneal injection of CP (10 mg/kg body weight) at the 10th day of experimentation. Biochemical studies were performed to evaluate kidney function; protein expression by Western blot and mRNA expression of related gene were studied from the kidney tissues to evaluate the effects of CFAR. Histopathological analysis was done to investigate the structural abnormalities and fibrosis of renal tissues.

Result: Our result reported that CFAR contain many bioactive phytochemicals having many pharmacological properties. Cell viability assay and assay of apoptosis reported that different doses of CFAR could reduced CP-induced cell death and cell apoptosis. The levels of kidney injury markers (BUN, sCr and eGFR), inflammatory markers (Interleukin-18, KIM-1, Cys-C, NF- κ B and NGAL), and antioxidant markers (SOD, GSH, CAT, Nrf2 and Bcl2) and lipid peroxidation (MDA) were settled to a normal level by the oral administration of high doses (100 and 200 mg/kg body weight) of CFAR after intraperitoneal injection of CP as suggested by biochemical, histopathological, protein and gene expression studies.

Conclusion: In conclusion, CFAR at the high doses (100 and 200 mg/kg body weight) could able to protect the kidneys from CP induced oxidative stress and inflammation due to presence of bioactive phytochemicals that prevent the activation of oxidative stress induced signalling cascades leading to kidney damage.

* Corresponding author. Nutrition Research Laboratory, Department of Paramedical and Allied Health Sciences, Midnapore City College, Kuturiya, Bhadutala, Midnapore, 721129, India.

E-mail addresses: janasahadeb71@gmail.com (S. Jana), pmitra664@gmail.com (P. Mitra), titlipanchali19@gmail.com (T. Panchali), aminakhatun158@gmail.com (A. Khatun), tridipdas30@gmail.com (T.K. Das), micro.kuntal@gmail.com (K. Ghosh), shrabanutrition@gmail.com (S. Pradhan), sudiptadna@gmail.com (S. Chakrabarti), suchismitaroy2011@yahoo.in (S. Roy).

<https://doi.org/10.1016/j.jep.2024.119084>

Received 4 July 2024; Received in revised form 30 October 2024; Accepted 8 November 2024

Available online 19 November 2024

0378-8741/© 2024 Elsevier B.V. All rights reserved, including those for text and data mining, AI training, and similar technologies.

1. Introduction

The rapid reduction in kidney function associated with acute kidney injury (AKI) can result in chronic kidney disorders, a global public health concern whose prevalence has been steadily rising (Meng et al., 2018). Renal replacement therapy comes at a significant expense to the health system, and the disease's progression to more severe stages is linked to high rates of morbidity and mortality, mostly from cardiovascular illnesses and diabetes. It is therefore critically necessary to discover promising pharmaceutical medicines to protect kidney function and prevent the progression of end-stage renal disease (ESRD).

One of the most often used animal models of experimental nephrotoxicity is cisplatin (CP)-induced AKI. The usual first-line treatment for a wide range of cancers, including head, neck, lung, ovarian, bladder, cervical, and testicular cancer, is CP, an efficient platinum-based chemotherapeutic drug. However, serious organ toxicities as nephrotoxicity, neurotoxicity, ototoxicity, and hepatotoxicity limit its clinical applicability (Sun et al., 2019). The CP treatment has a significant negative impact on the kidney's proximal tubules, particularly the S3 segment, which is characterized by nuclear chromatin condensation, cellular enlargement, and microvilli loss. The primary components of CP-induced AKI are inflammation, apoptosis, necrosis, oxidative stress, and reactive oxygen species (ROS) generation. Furthermore, in response to toxicity, autophagy is activated as a strong defense against kidney damage (Purena et al., 2018).

Reactive oxygen species are produced when a nephrotoxic drug causes oxidative stress. According to earlier research, CP-induced AKI is linked to an aggravation of the antioxidant status, which includes decreased levels of antioxidant enzymes including GSH, SOD, and catalase (CAT) in renal tissue as well as an increase in lipid peroxidation and its end product, malondialdehyde (MDA) (Ognjanović et al., 2012). A number of signaling protein pathways, including the inflammatory pathway of nuclear factor- κ B (NF- κ B), are activated by oxidative stress (Sahu et al., 2014). Nearly all animal cell types include the protein complex known as NF- κ B, which is responsible for DNA transcription and is involved in a number of activities, including inflammation, apoptosis, the immune system, cell proliferation, and development.

It has been proposed that the interaction between the nuclear factor erythroid 2-related factor 2 (Nrf2) and NF- κ B signaling pathways modulates the transcription or activity of target proteins downstream. The early stages of inflammation are likely when NF- κ B-mediated transcriptional activity is suppressed or inactivated through Nrf2. This is because NF- κ B controls the de novo synthesis of several pro-inflammatory mediators. Despite this, Nrf2 is connected to additional signaling pathways, including B-cell lymphoma 2 (Bcl-2). The most well-known protein family, the Bcl-2 family, is responsible for controlling the mitochondrial pathway, which in turn controls apoptotic cell death. Members of this family also break free from an oligomeric channel that allows cytochrome C from the mitochondrial intermembrane space to diffuse into the cytosol and activate caspase, which in turn causes apoptosis (Wang et al., 2020; Chipuk et al., 2010; Thimmulappa et al., 2006; Satta et al., 2017; Liu et al., 2009). According to a study, CP-induced AKI in rats elevated the mRNA and protein expression of a number of biomarkers, including kidney injury molecule-1 (KIM-1), interleukin-18 (IL-18), cystatin C (Cys C), and neutrophil gelatinase-associated lipocalin (NGAL). Within the immunoglobulin superfamily, KIM-1, also referred to as T cell immunoglobulin mucin domains-1, is a glycoprotein with an extracellular, transmembrane, and intracellular tail. KIM-1 is mostly elevated at the apical membrane of the proximal tubules in patients with acute or chronic renal impairment, despite the fact that it is almost undetectable in normal kidneys. The kidney's epithelial cells produce IL-18, a cytokine that promotes inflammation. It may contribute to the formation of renal cell fibrosis and is increased in chronic renal illness (Jana et al., 2022). Similar to this, the iron transporter protein NGAL is mostly expressed in the proximal tubules and, to a lesser degree, in the collecting ducts and

ascending limb of the loop of henle. Moreover, the production of NGAL implies that damaged kidneys discharge NGAL into the bloodstream, where it is subsequently eliminated by urine. Serum creatinine (sCr) and estimated glomerular filtration rate (eGFR) have a significant correlation with NGAL in the urine (Rysz et al., 2017; Chakraborty et al., 2012). All nucleated cells produce Cys-C, an endogenous biomarker of renal function that is a 13 kDa endogenous cysteine proteinase inhibitor. Cys-C is eliminated from circulation via glomerular filtration without reabsorbing or secretion. As a biomarker of renal function, it performs as well as or better than sCr in most cases of AKI. Evidence suggests that Cys-C may be able to detect renal impairment earlier than creatinine since it rises before sCr occurs during AKI (Zhang et al., 2011). In order to maintain sustainability and improve accessibility, the health care system should continuously seek to expand its knowledge base, develop novel, safe, and effective technologies, and lower the costs associated with managing AKI and its sequelae. The lack of specificity in current management of renal damage and its association with inadequate supportive care highlight the need for novel strategies. Lately, natural ingredients have become increasingly significant in the creation and discovery of novel medications.

Shatavari, or *Asparagus racemosus* (AR) in the Asparagaceae family, is a native of the Indian subcontinent and has long been valued for its many health benefits. Shatavari literally means "having a hundred spouses," and ayurvedic texts rightly state that it fortifies a woman to the extent that she can bear thousands of healthy offspring. Shatavari, known as the "Queen of Herbs" by Ayurveda, is known for enhancing fertility and symbolizing love and devotion. Its use to the treatment of women's health conditions is supported by ancient writings like as the Ashtang Hridayam and the Charak Samhita (Alok et al., 2013). It is clear from the Kashyap Samhita that shatavari supports maternal health and that it should be used appropriately as a galactagogue. According to Akhtar et al. (2024), AR roots are used in modern Ayurvedic practices to prevent ageing, increase longevity, impart immunity, improve mental function, vigor, and addvitality to the body. They are also effective as an appetizer, stomach tonic, aphrodisiac, astringent, anti-diarrheal, anti-dysenteric, anti-inflammatory, blood purifier, kidney problems, and throat complaints (Garde, 1970). Moreover, they are used in cases of chronic colic and dysentery (Bopana and Saxena, 2007). Many different biological activities have been found by the studies conducted on both the isolated principles and the whole extracts. These include as a nerve tonic (Venkatesan et al., 2005), hepatoprotective (Kamat et al., 2000), antitumor (Shao et al., 1996), antifungal (Shimoyamada et al., 1990), and prevention and treatment of gastric ulcers. Methanolic extract of AR roots was found to have substantial *in vitro* antibacterial effectiveness against *Salmonella typhi*, *Vibrio cholerae*, *Shigella dysenteriae*, and *Escherichia coli*, according to a study (Mandal et al., 2000). Antilithiatic effect of AR on ethylene glycol-induced lithiasis in male albino wistar rats was studied and oral administration of AR ethanolic extract reduce oxalate, calcium and phosphate ions in urine which are the main cause of renal stone formation (Sharma et al., 2011). Various bioactive phyto-compounds found in AR roots, such as tannins, alkaloids, terpenoids, steroids, and flavonoids, may have a distinct physiological influence on human health (Bopana and Saxena, 2007; Mitra et al., 2012; Singh et al., 2023). Use of this medicinal plant for the protection of kidney functions and preventing renal disorders were not investigated sufficiently earlier. Hence, this study aimed to determine the antioxidative and anti-inflammatory potentiality of AR roots and protective role of its chloroform fraction on CP induced renal toxicity by preventing the loss of renal function in experimental rats.

2. Materials and method

2.1. Chemicals and antibody

Dulbecco's Modified Eagle Medium Low Glucose (5.5 mM/L) medium, fetal bovine serum, 1% L-glutamine, 1% penicillin/streptomycin,

3-(4,5-dimethyl-2-thiazolyl)-2,5-diphenyl tetrazolium bromide (MTT) assay kit, acridine orange (AO) and ethidium bromide (EB), 4, 6-diamidino-2-phenylindole (DAPI) purchased from Himedia, India, CP was purchased from Sigma Aldrich, Quercetin, HPLC grade solvents and chemicals were obtained from Merck (Germany) and ThermoFisher. Enzyme-linked immunosorbent assay (ELISA) kits for KIM-1, Cys-C, IL-18, and NGAL were purchased from ELK Biotechnology, other chemicals for genomic and biochemical analysis were purchased from HiMedia and Merck. Primers for qPCR was obtained from Edison Life Science (India) and primary antibodies for Western blot were purchased from ABclonal (USA) and secondary antibody from AbgeneX (Bhubaneswar).

2.2. Preparation of AR roots fraction

Roots of AR were collected from local market of Midnapore town, West Bengal, India. Roots were washed, cuts, dried, grinded and then chloroform fraction were separated by earlier standardized method (Roy et al., 2018). To get removal of the oily non-polar components, 50 g of powdered root material was washed in 200 ml of hexane for 24 h. Hexane was discarded, and the remaining material was dissolved in hydromethanol (4:6 mixture of methanol and water) and placed for 2 h in a soxhlet apparatus. After that hydromethanol extract of AR roots were obtained. That extracts was further diluted in 250 ml of chloroform and again placed for another 2 h in the soxhlet apparatus. After that the whole content was filtered through Whatman No. 1 filter paper and the filtrate was evaporated through a rotary vacuum evaporator at 40 °C while under decreased pressure (Roy et al., 2018). The fraction, referred to as the CFAR, was kept in a refrigerator for further use. For oral feeding of the fraction, freshly prepared 1% carboxymethyl cellulose in distilled water was used as a vehicle (Kasali et al., 2022).

2.3. High performance liquid chromatography (HPLC) analysis of CFAR

High performance liquid chromatography of AR roots and standard quercetin were performed using an HPLC system of the Agilent 1260 Infinity II Quaternary LC, lab-solution software, UV-Visible detector set at 273 nm, and 10 µL sample and standard (1 mg/ml) was injected. All chromatographic analysis was carried out on an Agilent Poroshell 120 EC-C18 column (4.6 × 150 mm, 4 µm) with a guard column (Agilent, USA) performed at 35 °C and a flow rate of 0.5 ml/min. The mobile phase consisted of acetonitrile (mobile phase A) and methanol (B) was applied in a ratio of 1:1. The run time was 10 min. For calibrate, standard quercetin was prepared at different concentrations (10, 20, 50, 100, 200, and 300 µg/ml) using HPLC-grade methanol. The standard was presented in triplicate, and the mean detectable response was evaluated. All the samples and standard were filtered with the help of 0.45 µm filters (PES hydrophilic, Himedia and Vadhani, Mumbai, India) before injection (Sammani et al., 2021).

2.4. Liquid chromatography-mass spectrometry (LC-MS) analysis of CFAR

The LC-MS/MS system consisted of a Dionex Ultimate 3000 UHPLC chromatographic system and an ESI source-mass spectrometer (Thermo Fisher- Q Exactive) was used for the analysis. The system control and data analysis were performed by Lab Solutions software. Chromatographic separation was carried out on a Phenomenex, Kinetex, C18, 100 A, column (100 × 2.1 mm, 2.6µ). The UHPLC was operated with a gradient mobile phase system consisting of 10 mM ammonium acetate in water (0.1% formic acid) (phase A) and acetonitrile (0.1% FA) (phase B) at a flow rate of 0.1 ml/min: 0–2 min, 0.2 ml/min: 2.1–45 min, 0.1 ml/min: 45.1–55 min. The pump was programmed as follows: phase B was increased from 0 to 20% within the first 2.1–20 min, increased to 20–60% within the next 20–35 min, and increased to 60%–100% within the next 35–40 min, from 100% within the next 40–45 min then back to

0% within the 45.1–55 min (total gradient time: 55 min). A 10 µl of sample (CFAR) was injected into the system with the auto-sampler conditioned at 10 °C and column temperature maintained at 40 °C. The mass spectrometer was operated in an FS; DDS; positive and negative ion mode. Mass spray voltage (+ve) 4000v; mass vaporized temperature 280 °C; sheath gas flow rate was 30Arb; samples were diluted 100 times with methanol. The samples were centrifuged for 5 min. A 10 µl of the supernatant was injected for analysis (Quan et al., 2021).

2.5. In-vitro cell culture studies

2.5.1. Effect of CFAR in CP-induced toxicity in NRK-52E cells

Normal rat kidney (NRK-52E) cell line was acquired from National Centre for Cell Sciences (NCCS), Pune, India. The cells were cultured in Dulbecco's Modified Eagle Medium Low Glucose (5.5 mM/L) with 10% fetal bovine serum, 1% L-glutamine, and 1% penicillin/streptomycin (Himedia) at 37 °C in a 5% CO₂ incubator. The cells were grown till 80–90% confluency, after which they were used for experiments. The cells with 70–80% confluency were trypsinized and sufficient media added to inactivate the trypsin activity. The cells were centrifuged at 1200 rpm for 10 min, supernatant was discarded and resuspended the pellet in media prior to counting on a haemocytometer by methylene blue exclusion method. The cells were diluted in media to get desired number of cells. For cell growth studies, the final seeding density was kept 10,000 cells/well in a 96-well flat bottomed microtiter plate. Post 24 h of cells seeding, cells were untreated, treated with CP and cotreated with CP (20 µM) and CFAR (5, 25, 50, 100, 200 and 400 µg/mL) for 24 h. After 24 h of treatment, cell viability assay and cell morphological analysis were performed.

2.5.2. Cell viability and dose determination of CFAR using MTT assay

Using MTT assay, different concentration of CFAR was used to treat the NRK 52 E cells at first to determine any toxic effects. In brief, 10,000 cells were seeded in a 96-well plate. After 24 h, cells were exposed to different concentrations CFAR along with an untreated control well, for 24 h. After treating them for 24 h, 10 µL of MTT solution was added to each well at a final concentration of 0.5 µg/mL and the cells were incubated at 37 °C in a 5% CO₂ atmosphere for 3 h in the dark. Following the incubation period, formazan crystals formed in each well were solubilized using 100 µL dimethyl sulfoxide (DMSO) solution. The absorbance was then measured at 570 nm to determine the viability of cells. Similar to that effect of CFAR at different doses on CP induced nephrotoxicity was determined by this method.

2.5.3. Assay of apoptosis parameters

The NRK-52E cells were treated with CP (20 µM) and different concentrations of CFAR (5, 25, 50, 100, 200 & 400 µg/ml), and they were collected and adjusted to 10⁶ cells/ml. The AO and EB solution were added to cell suspension and incubated for 15 min at room temperature. The cells were observed under the fluorescence microscope (Lateef et al., 2023).

2.6. Acute toxicity study of CFAR

The acute toxicity study of CFAR was evaluated in 35 rats. All rats were divided into seven groups; each group contained five rats. After that rats were fasted for 24 h and single dose of CFAR was orally fed in the following manner: 50, 100, 200, 500, 1000, 2000, 3000 mg/kg body weight (bw) according to OECD guideline 423 (OECD, 2002). After the dosing, the rats were observed for wellness parameters and recorded up to 15 days for changes in skin and fur, eyes, mucus membrane, behavioral pattern changes, tremor, convulsions, salivations, diarrhea, lethargy, sleep and mortality. As no changes and complication were arises so, three different doses (50, 100 and 200 mg/kg) were chosen for further experimentation.

2.7. Animal selection and treatment

Prior to conducting any animal research, the Midnapore City College institutional animal ethics committee (2256/PO/Re/S/23/CCSEA) provided approval. A total of thirty-six male albino rats of the wistar strain, weighing around 150 ± 5 g, had been purchased from Saha Enterprise in Kolkata. They were housed in a controlled environment that had a 12-h light/dark cycle, a temperature of 24 ± 2 °C, and a humidity of $50 \pm 5\%$. The rats were housed in hygienic polypropylene cages with no restrictions over food and sterile water. The animals were divided up into six groups, each with six rats.

Group I was designated as the control group, receiving adequate amount of water and standard food. Group II was the vehicle control (VC) group, receiving 200 mg/kg of CFAR for 15 days. Group III was the AKI group, receiving a single intraperitoneal injection of CP at a dose of 10 mg/kg body weight. Group IV, V, and VI were given CFAR orally for 15 days at 50, 100, and 200 mg/kg body weight/day respectively, following which they received a single intraperitoneal injection of CP on the tenth day of the experiment. All of the animals had been sacrificed after a total of 15 days of investigation; prior to this, urine was collected in order to analyze the urinary profile for AKI. Following scarification, kidney and blood samples were taken for studies concerning mRNA expression, protein expression, histopathology, and biochemistry as well.

2.8. Measuring body weight and assessment of renal somatic index

We started by using an automated weighing balance to determine each animal's initial body weight. Then, we collected data each day leading up to scarification and documented each animal's ultimate body weight. Rats' Naso-anal length was measured to determine their eGFR, and kidney weight following scarification was used to calculate their renal somatic index (do Nascimento et al., 2013; Jana et al., 2023).

2.9. Biochemical assay for renal function

Blood samples were obtained for separating serum, which was then centrifuged for 30 min at 3000 rpm after being stored at room temperature for an hour. Using commercial kits (Coral, India), the biochemical test of sCr and BUN was measured in accordance with the manufacturing specifications for Berthelot and Jaffe's techniques, respectively. The Schwartz equation was used to determine eGFR indirectly from sCr, and rat height: $eGFR = \text{height (cm)} \times k/sCr$, with $k = 0.55$ (Alorabi et al., 2022).

2.10. Assessment of oxidative and anti-oxidative indicators

Renal oxidative and anti-oxidative parameters were measured by UV-Vis spectrophotometer. The antioxidant activities of GSH, SOD and CAT activity was determined spectrophotometrically and recorded. MDA levels in kidney tissue homogenate was measured as previously established method (Atessahin et al., 2005).

2.11. Evaluation of inflammatory cytokines

ELISA kits were used to measure the level of urinary Cys-C, KIM-1, NGAL and IL-18 according to the manufacturer's instructions (ELK biotechnology, Wuhan).

2.12. Profile of gene expression using quantitative polymerase chain reaction (qPCR)

Kidney tissues were used to extract total RNA using TRIzol (Life Technologies). Using a NanoDrop 2000c Bio spectrophotometer, the concentration of RNA was found. A high-capacity cDNA extraction kit (Applied Biosystems, Foster City, CA, USA) was used to reversely

transcribe 1 µg of total RNA for each RNA sample. Using qPCR, target gene expression for primer profiles (Table 1) were examined. The processes involved in PCR were as follows: first, denaturing DNA at 95 °C for 5 min; second, denaturing DNA at 95 °C for 30 s; third, annealing DNA at 62 °C for 45 s; fourth, extension of DNA at 72 °C for 1 min and last, extending DNA at 72 °C for 5 min. The second and third phases were repeated for a total of 37 thermal cycles. Finally, the sample-containing PCR tube was kept at 4 °C.

Next, utilizing glyceraldehyde 3-phosphate dehydrogenase (GAPDH) as a housekeeping gene, the GeNei™mini-submarine gel technique was utilized to examine the gene expression of KIM-1, IL-18, Cys-C, NGAL, NF-κB, Nrf2, and Bcl-2. Using the GeNei™mini-submarine gel technique, 5 µL of the PCR product were combined with 1 µL of sample loading dye and 5 µL of DNA size standard 3000. The amplified fragments were divided into groups based on the molecular sizes of each group. Using the gel documentation imaging system, the results were analyzed. Following that, densitometry analysis was performed using ImageJ software with GAPDH normalization in order to measure the DNA bands on the gels (Stael et al., 2022).

2.13. Analysis of mRNA expression by real-time quantitative reverse transcription polymerase chain reaction (qRT-PCR)

KIM-1, IL-18, Cys-C, Nrf2, NF-κB, and Bcl-2 gene expression were assessed using real-time quantitative reverse-PCR using an Agilent G8830A AriaMx system with SYBR Green detection assays. The house-keeping gene GAPDH was used to standardize the target gene's expression levels. Gene-specific primers (1 µl) were used to assess the expression of each gene. To 1 µl of cDNA sample, 10 µl of Brilliant III ultra-fast SYBR Green qPCR Master Mix (Agilent, USA) was added. Using water suitable for molecular biology, adjust the total volume to 20 µl. The following procedures were used to carry out the PCR reactions utilizing thermal profile RT-PCR: initial denaturation at 95 °C for 1 min, denaturation at 95 °C for 30 s, annealing at 59 °C for 45 s, extension at 72 °C for 2 min, and final extension at 72 °C for 10 min. A total of 37 thermal cycles were performed by repeating steps 2 and 3. Finally, the PCR tube containing the material was stored at 4 °C. The target gene expression fold change was calculated using the $2^{-\Delta\Delta CT}$ threshold technique and normalized to the controls (Livak and Schmittgen, 2001).

2.14. Western blot analysis to evaluate protein expression

Western blotting was used to analyze the expression of specific proteins in kidney tissue. The first step involved homogenizing the tissues using radio immunoprecipitation assay (RIPA) buffer, which functions as a promising cell lysate. The Lowry method was then used to measure the amount of protein. The 50 µg protein sample was measured and then added to the loading buffer. The material was boiled for 5 min before being transferred to a nitro-cellulose membrane (Bio-Rad) for SDS-PAGE electrophoresis. To the membrane 4% bovine serum albumin was added to block it, and was incubated with primary antibody at 4 °C for the whole night. The primary antibodies used in this investigation were from Affinity Bioscience and ABclonal consisted of β-actin, KIM-1, IL-18, NGAL, NF-κB, Nrf2, and Bcl-2 at a 1:1000 ratio. After that, the

Table 1
Primer profile of specific gene sequence used in this experiment.

Gene	Forward primer (5'-3')	Reverse primer (5'-3')
KIM-1	GAGGCCTGGAATAATCACAC	AATCTCCCAGGAGCTGGAAT
IL-18	AAGACCAGCCTGACCCACAT	ACCCGTGTGTGTCGTTTTGA
NGAL	GACAACCAATCCAGGGGAAG	GCATACATCTTTTGGGGTCT
Cys C	GCCTGTGCCTATCACCTCTTAT	CCTTCTCTGTCGTCTCTGGT
NF-κB	GACAGTGACAGTGTCTGCGA	AGTTAGCAGTGAGGCCACCAC
Nrf2	CATTGTAGATGACCATGAG TCGC	ATCAGGGGTGGTGAAGACTG
Bcl2	GACAGAAGATCATGCCGTCC	GGTACCAATGGCACTTCAAG
GAPDH	CGCTGGTGCTGAGTATGTCC	CTGTGGTCATGAGCCCTTCC

membrane was incubated for 60 min at 4 °C with an HRP-labeled secondary antibody 1:7500 (Abgenex) after being washed three times with phosphate buffer saline with tween-20. With the use of 3,3',4,4'-Tetraaminobiphenyl tetrahydrochloride, certain protein bands were identified (Chakrabarti et al., 2018).

2.15. Densitometric analysis

With the aid of software, densitometric analysis was used to quantify the DNA bands on the gel. The density of the bands on the agarose gel was compared using ImageJ software in this instance. The bands' mean area value was displayed together with the rectangular area of every single band. The same area was chosen for each band in order to compare the band densities on an agarose gel. The gene of interest (Table 1) was divided by the housekeeping gene (GAPDH) after the mean density value of all the bands has been presented in excel (Stael et al., 2022). β -actin was used as an internal reference and the band on the nitrocellulose membrane was quantified using the same technique and software to determine the protein reactivity.

2.16. Histopathological assessment of rats kidney tissues

Kidney tissue slices (4 μ m) were obtained from each group of experimental rats, fixed, processed, and paraffinized. The tissue sections were subjected to light microscopy examination after being stained with hematoxyline and eosine (H&E) and periodic acid-Schiff (PAS) staining,

respectively (Khairnar et al., 2024). Through blind evaluation of these slices, a nephrologist and a renal pathologist determined the degree of histological modification in tubular and glomerular damage, including necrosis, cell loss, tubular dilatation, fibrosis, and necrotic casts, using a semiquantitative scale. The scale had four categories: 0, normal kidney; 0.5, less than 10%; 1, 10–25%; 2, 25–50%; 3, 50–75%; and 4, 75–100% (Lin et al., 2017).

2.17. Statistical analysis

Statistical analysis was performed using Graphpad Prism 8.0 software. All values were expressed as mean \pm SE student's t-test was used between two groups and two-way analysis of variance (ANOVA) was used for statistical analysis. ANOVA was followed by Tukey's multiple comparison test. The results were considered significant if $p < 0.05$.

3. Results

3.1. Identification of compound by HPLC analysis against standard

The solution of CFAR sample was chromatographed and obtained the concentration of quercetin of CFAR sample by using the regression equation. In the presently research, the HPLC process become used to study and quantify the flavanoids (quercetin) component from CFAR. The HPLC fingerprints of CFAR roots has shown one major peak at retention time 3.471 and minor peak at 2.38, 3.04, 3.98, 4.17, 4.44, 4.55, 5.89, 6.10, 8.86,

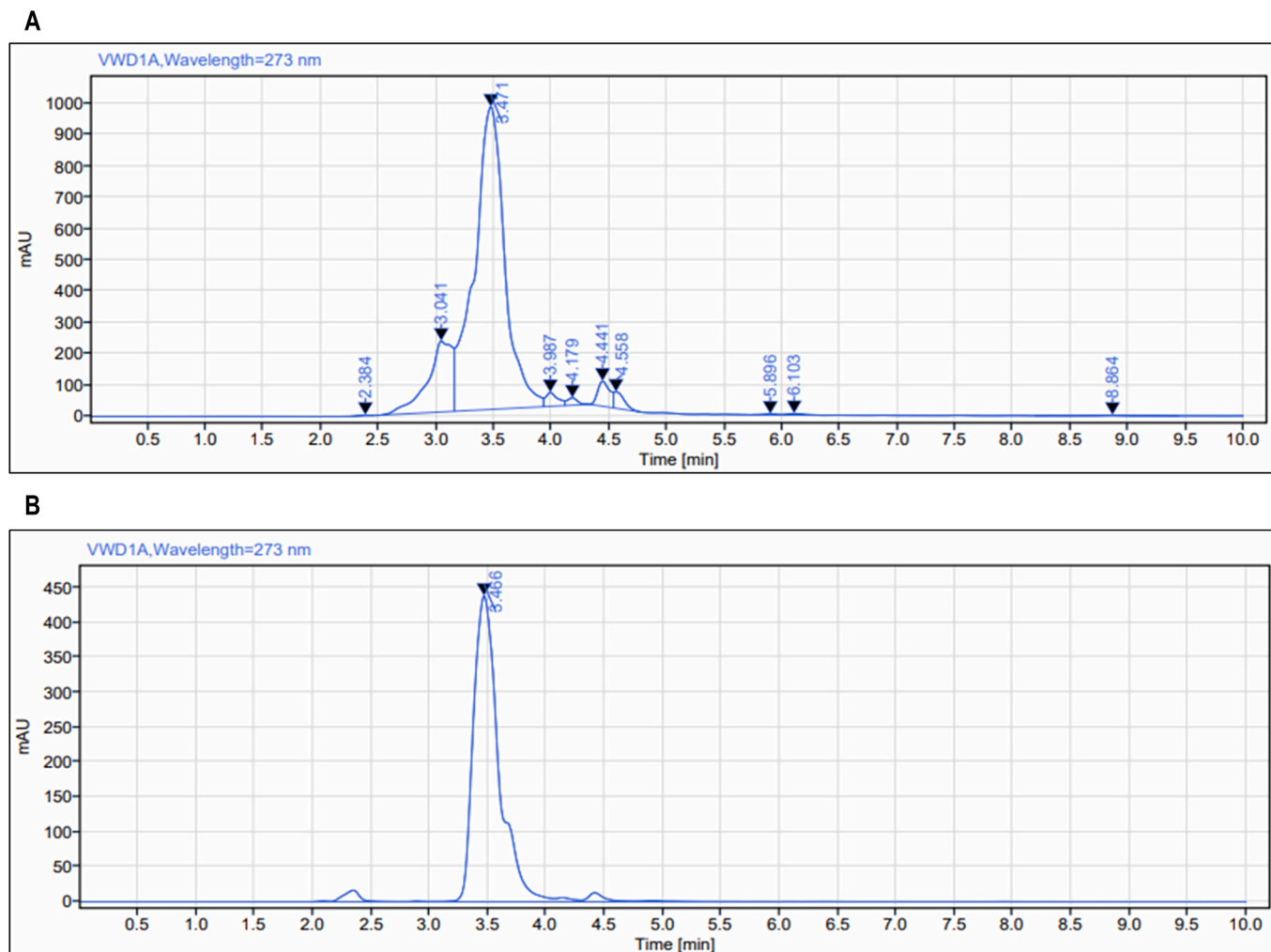


Fig. 1. HPLC analysis of chloroform fraction of *Asparagus racemosus* (A) and standard quercetin (B).

4.55, 5.89 and 6.10. Quercetin showed a major peak with retention time 3.46 (Fig. 1A and B) at the wavelength of 273 nm.

3.2. Preparation of the calibration curve of quercetin

For the preparation of calibration curve, different concentration (10, 20, 50, 100, and 300 µg/ml) of standard quercetin and CFAR (1 mg/ml) was prepared in methanol and run the HPLC as per the standard procedure mentioned earlier. After that mean peak area of standard and sample was calculated and plotted into curve. The regression equation was figured out on the basis of the curve. The calibration curve was used to compare the results obtained from the HPLC analysis of CFAR. The calibration curve of quercetin showed a linear relationship over all the used concentrations ($R^2 = 0.9988$). The linear regression equation for the curve was $y = 101.41x - 315.01$, where y is the ratio of peak area of flavonoids and x is the flavonoid concentration (µg/ml) (Fig. 2).

3.3. Characterization of phytochemicals using LC-MS analysis

LC-MS analysis was performed to characterize the major bioactive phytochemicals present in the CFAR. The results indicate that this fraction contain many bioactive phytoconstituents like 4-Oxo-L-isoleucine, flavone, D-pantothenic acid, syringic acid, orientin, bianthrone, cathine, apigenin, resveratrol, azafrin, isoarborinol, curcumin, β-sitosterol with the retention time 2.4, 7.5, 12.1, 13.0, 21.5, 25.5, 30.1, 32.8, 33.04, 35.9, 37.6, 39.5, 44.3 respectively (Fig. 3 and Table 2) as the data obtained from both the positive and negative ionization mode. Among these many compounds were not studied earlier for their nephroprotective potentialities though other pharmacological properties were already established by other researchers that were mentioned here (Table 2). So, these compounds may possess promising nephroprotective properties against CP induced AKI.

3.4. Effect of CFAR on CP-induced toxicity in NRK-52E cells

The efficacy of the CFAR was evaluated in CP induced cytotoxicity in NRK-52E cells by MTT assay. Cell viability was evaluated to assess the cytoprotective effect of CFAR in CP treated NRK-52E cells. NRK-52E cells were treated with various concentrations of CFAR (5, 25, 50,

100, 200 and 400 µg/mL) alone or in combination with CP (20 µM) for 24 h. Treatment with CFAR alone did not induce any overt detrimental effect on cell viability. Cell viability was significantly improved when CP induced cells were treated with CFAR. The EC_{50} was determined to be 7.94 µg/mL (Fig. 4). Treatment of CP significantly ($P < 0.001$) reduced the cell viability and was associated with morphological changes such as cell shrinkage, rounded cell shape and cytoplasmic vacuolation compared to normal control.

3.5. Effect of CFAR on apoptosis of NRK-52E cells

Apoptosis of NRK-52E cells was examined using the fluorescence microscope after staining the cells with AO/EB. Green live cells with normal morphology were observed in control group. NRK 52E cells treated with CP at the dose of 20 µM showed cell shrinkage, nuclear fragmentation and membrane blebbing. Treatment with different doses of CFAR (5, 25, 50, 100, 200 & 400 µg/ml) to the CP treated cells showed live cells with bright green nuclei and distinct chromatin structures specially to the 100, 200 & 400 µg/ml & were easily differentiated from CP treated apoptotic NRK-52E cells. Early apoptotic NRK-52E cells displayed green nucleus with chromatin condensation, whereas late apoptotic NRK-52E cells are stained orange and showed fragmented DNA with formation of beads in the nucleus (Fig. 5).

3.6. Effect of CFAR on body weight and renal somatic index

The initial and final body weights of each of the experimental animals were recorded. As depicted in Table 3 it was showed that there was significant ($p < 0.05$) decreased in body weight and increased renal somatic index for CP treated group III animals when compared to control. Orally feeding high doses of CFAR (100 and 200 mg/kg bw) to the CP treated animals (group V and VI) showed significantly ($p < 0.05$) increased in body weight and decreased renal somatic index as compared to group III animals. However, the lower dose of CFAR i.e. 50 mg/kg bw was not effective to provide nephroprotection to the CP treated rats (group IV) and thereby unable to maintain a control like body weight and renal somatic index (Fig. 6).

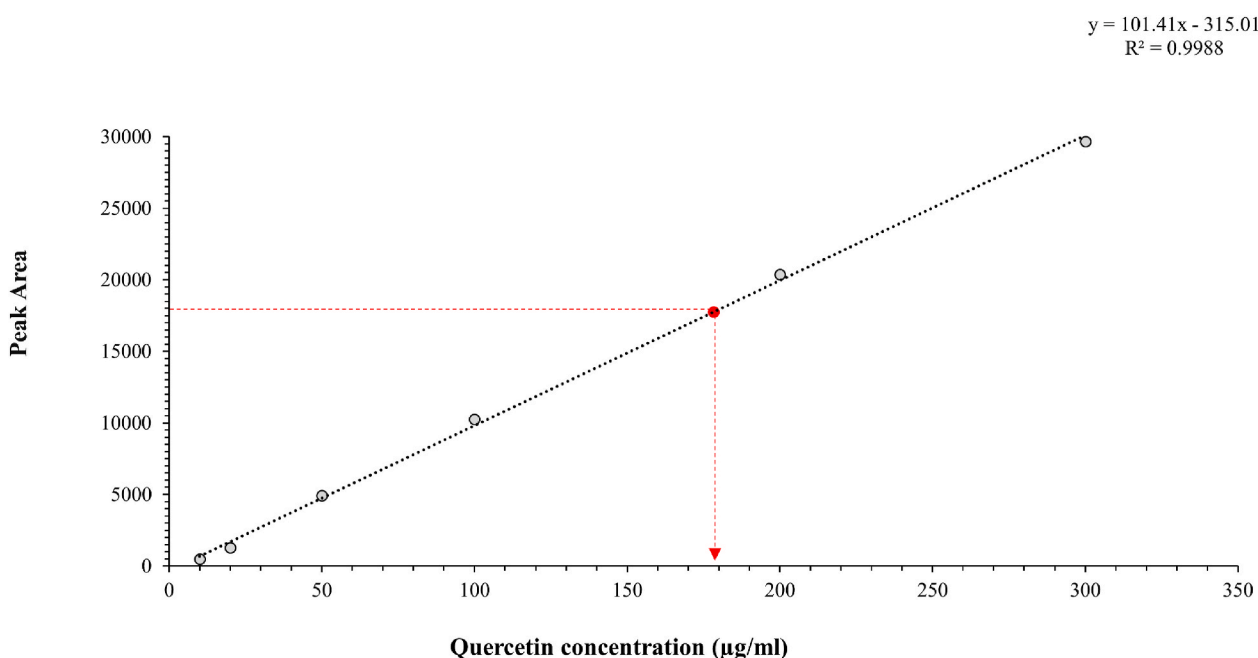


Fig. 2. Calibration curve of the quercetin.

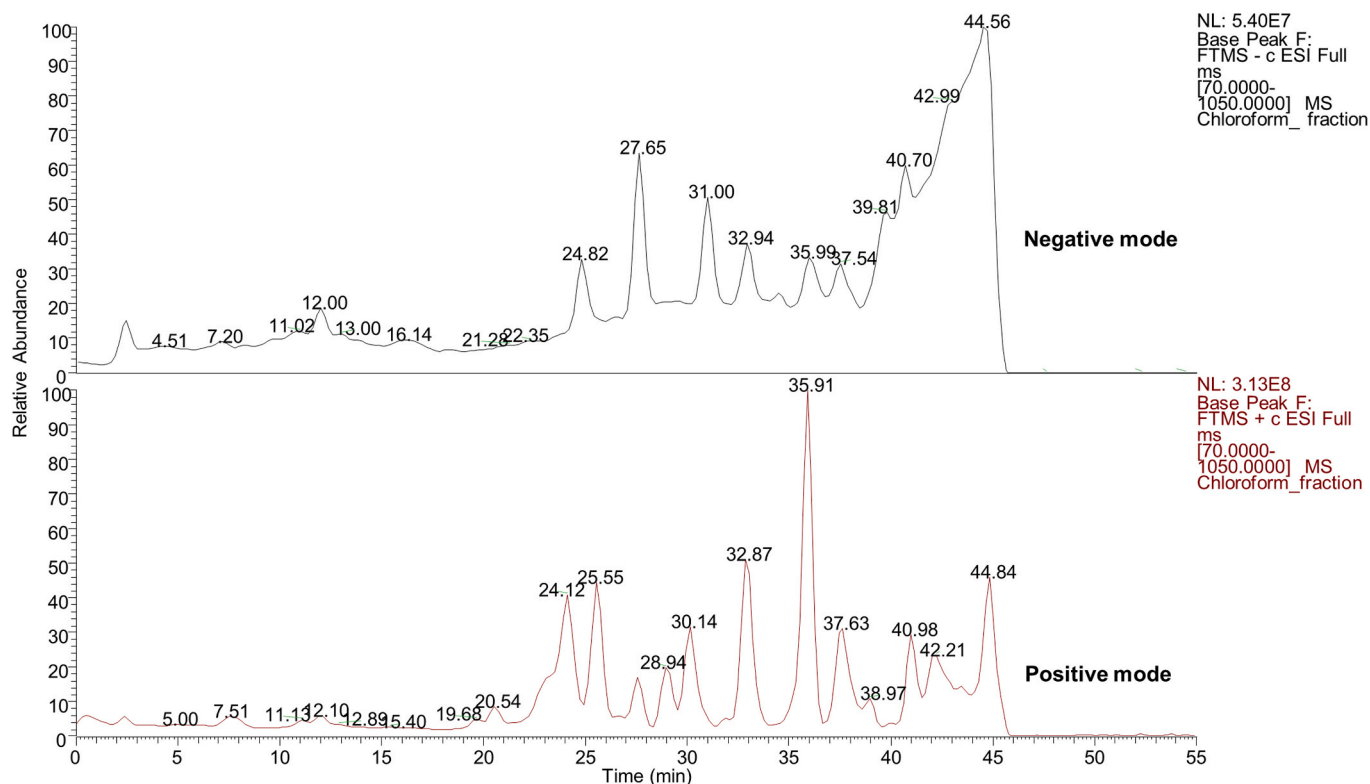


Fig. 3. LC-MS analysis of chloroform fraction of AR roots in both positive and negative ionization mode.

Table 2

List of possible bioactive phytochemicals present in the chloroform fraction of *Asparagus racemosus* roots as analyzed by LC-MS.

SL. No.	Retention time (min)	Name of suggested compounds	Molecular mass (g/mol)	Molecular formula	Pharmacological properties
1.	2.4	4-Oxo-L-isoleucine	145.07	C ₆ H ₁₃ NO ₃	It has been considered to be effective for insulin resistance, diabetes, obesity, lipotoxicity mitigation and liver function improvement (Avalos-Soriano et al., 2016).
2.	7.5	Flavone	222.06	C ₁₅ H ₁₀ O ₂	Flavone have antioxidative and anti-inflammatory properties that help to enhance the cellular microenvironment (Jiang et al., 2016).
3.	12.1	D-pantothenic acid	219.11	C ₉ H ₁₇ NO ₅	It may prevent the hypothalamic obesity (Naruta and Buko, 2001).
4.	13.0	Syringic acid	198.17	C ₉ H ₁₀ O ₅	It have antioxidant, anti-inflammatory properties which helps to treat neurological disorder (Ogut et al., 2022), modulating colorectal cancer (Mihanfar et al., 2021).
5.	21.5	Orientin	448.38	C ₂₁ H ₂₀ O ₁₁	Its antioxidative, antiaging, antiviral, anti-inflammatory, vasodilation, cardioprotective, radioprotective, neuroprotective, antiadipogenesis, and antinociceptive activities might lead to a potential therapeutic impact (Lam et al., 2016).
6.	25.5	Bianthrone	384.11	C ₂₈ H ₁₆ O ₂	The strong affinity of martianines for the GAPDH enzyme offers potential for developing novel medications to treat Chagas disease (Macedo et al., 2009).
7.	30.1	Cathine	151.09	C ₉ H ₁₃ NO	It serve as a weight-loss induced agent in obese people (Hauner et al., 2017).
8.	32.8	Apigenin	270.05	C ₁₅ H ₁₀ O ₅	It could regulate diabetes, obesity, depression, insomnia, infection, as well as protects respiratory, cardiovascular, liver functions, used to treat neurodegenerative disorders, and an useful candidate for managing inflammatory diseases (Mushtaq et al., 2023).
9.	33.04	Resveratrol	228.25	C ₁₄ H ₁₂ O ₃	It has anti-inflammatory, anti-carcinogenic, antioxidant, cardioprotective, viscoelastic, phytoestrogenic, antiaging, and immunomodulatory, antidiabetic, neuroprotective activities. It was commonly employed to treat stomach discomfort, urinary tract infections, hepatitis, arthritis, fungal illness, and skin inflammation (Zhang et al., 2021; Mitra et al., 2024).
10.	35.9	Azafrin	426.27	C ₂₇ H ₃₈ O ₄	It was attenuated myocardial injury through Nrf2-ARE pathway (Yang et al., 2018).
11.	37.6	Isoarborinol	426.38	C ₃₀ H ₅₀ O	Its anti-inflammatory properties were demonstrated utilizing a carrageenan-based edema model (Pham et al., 2023).
12.	39.5	Curcumin	368.38	C ₂₁ H ₂₀ O ₆	It has been utilized for protection or treat cardiovascular disease, respiratory illnesses, cancer, neurodegeneration, infections, and inflammation (Fu et al., 2021).
13.	44.3	β-sitosterol	414.70	C ₂₉ H ₅₀ O	It has numerous actions such as anti-inflammatory, antibacterial, antifertility, angiogenic, antioxidant, anticancer, antidiabetic, and antinociceptive, immunomodulatory activities (Ambavade et al., 2014).

3.7. Effect of CFAR on renal functional markers

As demonstrated in Fig. 7A–C, a significant ($p < 0.05$) elevation in BUN, sCr and eGFR level were observed in the CP treated animals when

compared to the control group which indicates decreased renal functionality that is occurred due to CP induced nephrotoxicity. These conventional kidney injury markers were noticeably ($p < 0.05$) decreased to the CP treated rats when CFAR was orally fed at 100 and 200 mg/kg

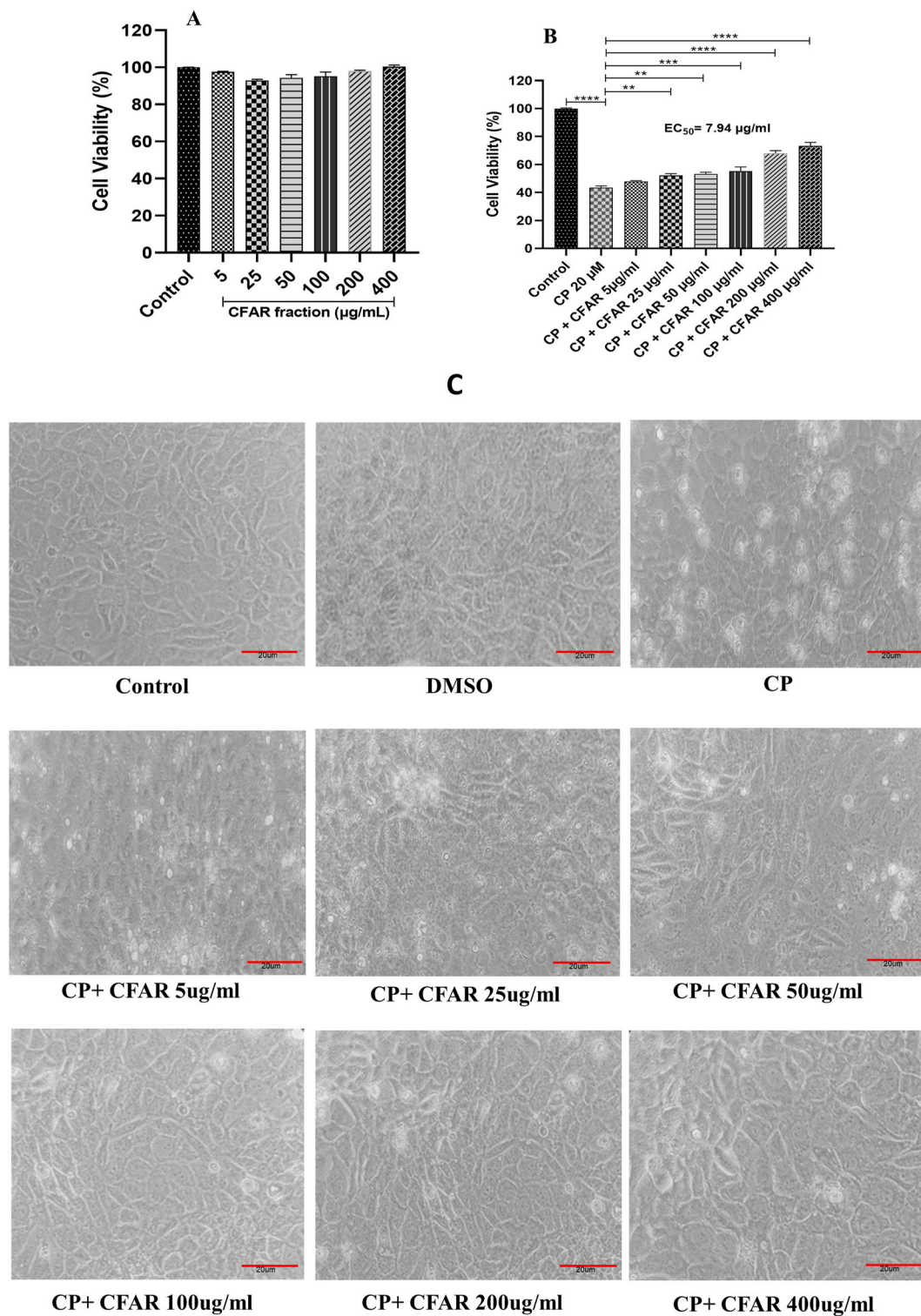


Fig. 4. Protective effect of CFAR in cisplatin (CP)-induced toxicity in NRK-52E cells. NRK-52E cells were treated with CFAR (5–400 µg/mL) for 24 h, followed by MTT assay (A). NRK-52E cells were treated with CP (20 µM) and CFAR fraction at different concentration (5–400 µg/mL) for 24 h and cytotoxicity was assessed using MTT assay (B). The data were presented as mean ± SE (n = 6) by two-way analysis of variance (ANOVA) followed by Tukey’s multiple comparisons test, where * p < 0.05, **p < 0.01, ***p < 0.001, ****p < 0.0001. Microscopic images of NRK-52E cell morphology with CP and CP + CFAR for 24 h (Magnification 40x) (C).

bw/day for 15 days. CFAR at the dose of 50 mg/kg bw could not provide nephroprotection and can’t able to maintain a normal level of BUN, sCr and eGFR level to the CP treated AKI rats.

3.8. Effect of CFAR on renal redox markers

The levels of GSH, SOD and CAT was significantly (p < 0.05) reduced in the kidney tissues of the CP induced nephrotoxic rats as compared to control. However, treatment with CFAR roots at the high doses i.e. 100 mg and 200 mg/kg bw/day for 15 days results significantly (p < 0.05)

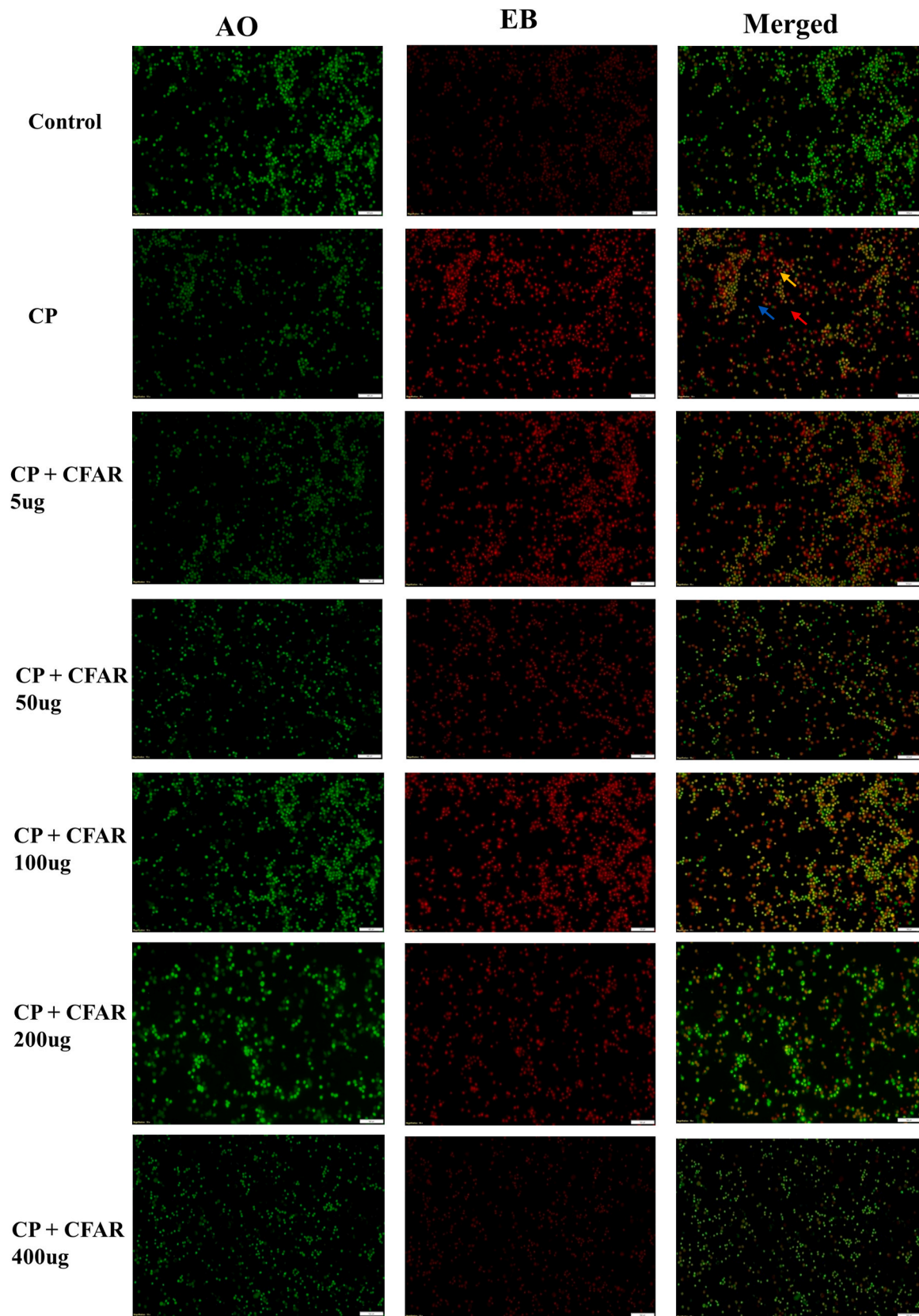


Fig. 5. Apoptotic morphology by AO/EB staining on NRK-52E cells treated with CP and CFAR (5–400 $\mu\text{g}/\text{ml}$) concentrations. Green viable cells show normal nucleus morphology; early apoptotic cells show bright green nuclear margination and chromatin condensation. Late apoptotic cells showed fragmented orange chromatin and apoptotic bodies. VC = viable cells (red arrow), EA = early apoptotic cells (yellow arrow), LA = late apoptotic cell (blue arrow). (For interpretation of the references to colour in this figure legend, the reader is referred to the Web version of this article.)

Table 3

Effect of CFAR on changes in the body weight against CP induced nephrotoxicity in rats at different dose-dependent study, length of all the experimental rats was recorded also.

Groups	Initial body weight (g)	Final body weight (g)	Difference (Initial - Final) (g)	Length (cm)
Control	154.35 ± 1.43	177.604 ± 1.82	+23.25 ± 1.62	19.44 ± 0.88
VC (CFAR)	157.19 ± 1.44	181.88 ± 1.39	+24.68 ± 1.88	20.85 ± 1.13
CP	156.79 ± 1.66	150.57 ± 2.02	-6.23 ± 1.39****	18.26 ± 1.03
CP + CFAR 50 mg/Kg BW	152.39 ± 2.55	156.96 ± 2.15	+4.56 ± 1.13*	18.45 ± 0.80
CP + CFAR 100 mg/Kg BW	150.15 ± 2.27	159.38 ± 2.45	+9.22 ± 0.74***	19.79 ± 1.10
CP + CFAR 200 mg/Kg BW	160.79 ± 1.94	178.13 ± 2.46	+17.33 ± 1.83***	20.21 ± 1.23

- Decrease; + Increase.

Data expressed as mean ± SE (n = 6). Multiple two tail t tests were carried out following an ANOVA (*p < 0.05, **p < 0.01, ***p < 0.001, ****p < 0.0001).

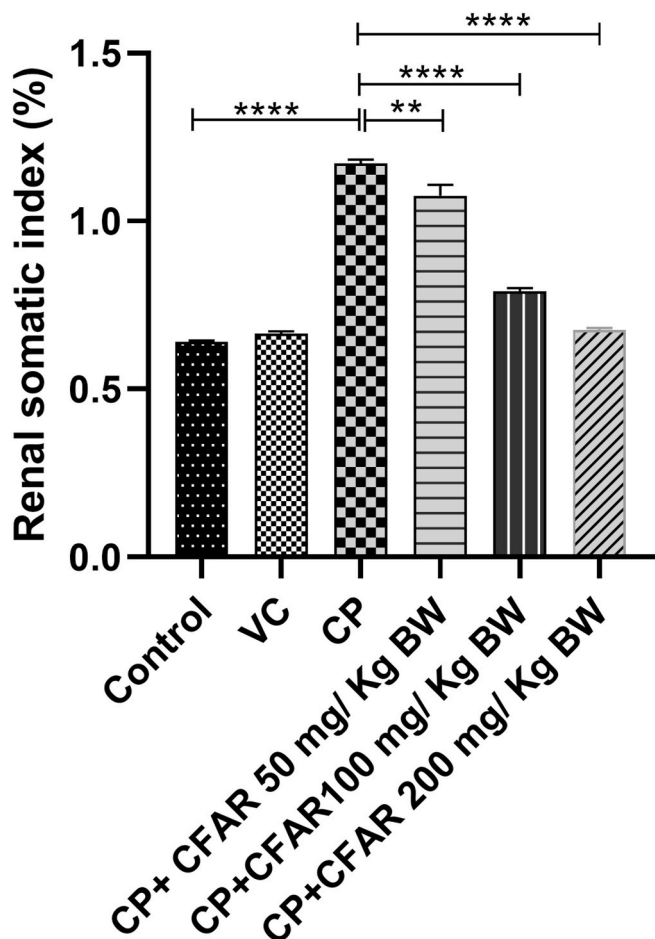


Fig. 6. Effect of CFAR on the renal somatic index of CP induced AKI. The data were presented as mean ± SE (n = 6) by two-way analysis of variance (ANOVA) followed by Tukey's multiple comparisons test, where * p < 0.05, **p < 0.01, ***p < 0.001, ****p < 0.0001.

increased level of these antioxidants in the kidneys compared to the CP induced group III rats. On the other hand level of these antioxidant enzymes were found to be significantly (p < 0.05) very low for the

animals treated with the low dose of CFAR at 50 mg/kg bw/day. Our results indicated that CFAR roots at the high doses (100 and 200 mg/kg bw) could protect the kidney functions against damage from oxidative stress and inflammation caused by CP. Furthermore, Fig. 8D indicated that a key lipidperoxidative marker, MDA in kidney tissues was significantly (p < 0.05) elevated in CP treated group compared with control group. Orally administration of CFAR at 100 and 200 mg/kg bw could significantly (p < 0.05) reduced the MDA level when compared to CP treated group III rats (Fig. 8A–D).

3.9. Effect of CFAR on kidney inflammation

Results showed that, the urinary levels of KIM-1, IL-18, NGAL and Cys-C were significantly (p < 0.05) increased in CP treated animals compared to control. Treatment with the high doses of CFAR i. e. 100 and 200 mg/kg bw/day for 15 days could be able to protect the renal function by maintaining the tubular structural integrity, prevents inflammation and thereby significantly (p < 0.05) low level of these urinary biomarkers were observed. The results indicated that CFAR roots at the dose of 100 and 200 mg/kg bw might be reduced the synthesis and released of inflammatory cytokines in the urine of the CP-induced AKI rats (Fig. 9A–D).

3.10. Effect of CFAR on relative mRNA expression in kidney tissues

Results suggested that the mRNA expression of KIM-1, IL-18, Cys-C, NGAL and NF-κB were significantly (p < 0.05) upregulated to the CP treated animals compared to the control group. Orally feeding of CFAR at high doses (100 and 200 mg/kg bw) to the CP treated group V and VI animals there was downregulation of these mRNA levels compared to CP treated group III animals. Moreover, the renal expression of Nrf2 and Bcl2 was significantly (p < 0.05) downregulated in CP treated group as compared to control, however rats orally fed with CFAR roots at the dose of 100 mg and 200 mg/kg bw for 15 days resulted in marked upregulation in the mRNA expression of Nrf2 and Bcl2 in kidney tissues. The lower dose of CFAR i.e. 50 mg/kg bw could not able to prevents the renal tissue damage and thereby there was no significant changes observed when compared with CP treated group III animals (Fig. 10A–H).

Furthermore, mRNA expression study by qRT-PCR was used to compute the fold change in targeted gene expression, which was then normalized to the controls as confirmatory analysis for KIM-1, IL-18, Cys C, NF-κB, Nrf2 and Bcl2. With the orally feeding of CFAR at 100 mg and 200 mg/kg bw to the CP treated group V and VI animals mRNA expression level of KIM-1 (1.14-fold and 1.46-fold), IL-18 (2.22-fold and 0.93-fold), Cys-C (1.39-fold and 1.05-fold), NF-κB (0.57-fold and 0.49-fold) was significantly (p < 0.05) downregulated as compared to the CP treated group III rats. Figure showed that the mRNA expression level of Nrf2 (0.34-fold) and Bcl-2 (0.45-fold) was significantly (p < 0.05) down-regulated in the CP-induced AKI group as compared to the control group. However, rats orally fed with CFAR roots at the dose of 100 mg and 200 mg/kg bw for 15days resulted in marked upregulation in the mRNA expression of Nrf2 (1.59-fold and 1.44-fold, p < 0.05) and Bcl-2 (4.30-fold and 5.05-fold, p < 0.05) in kidney tissues as compared to the CP treated group III animals. Our findings showed that high doses of CFAR treated rats may be prevent mRNA expression levels of CP-induced AKI models. Result of the related mRNA expression ensures that bioactive phytochemicals present in the CFAR could possess nephroprotective properties and thereby prevents DNA damage and helps to maintain normal kidney functioning (Fig. 11A–F).

3.11. Effect of CFAR on protein expression in kidney tissues

Analysis of protein expression for KIM-1, IL-18, NGAL and NF-κB was significantly (P < 0.05) upregulated in kidney tissue of CP treated group III animals compared to control group as detected by western blotting. The protein expression levels of these relative markers was significantly

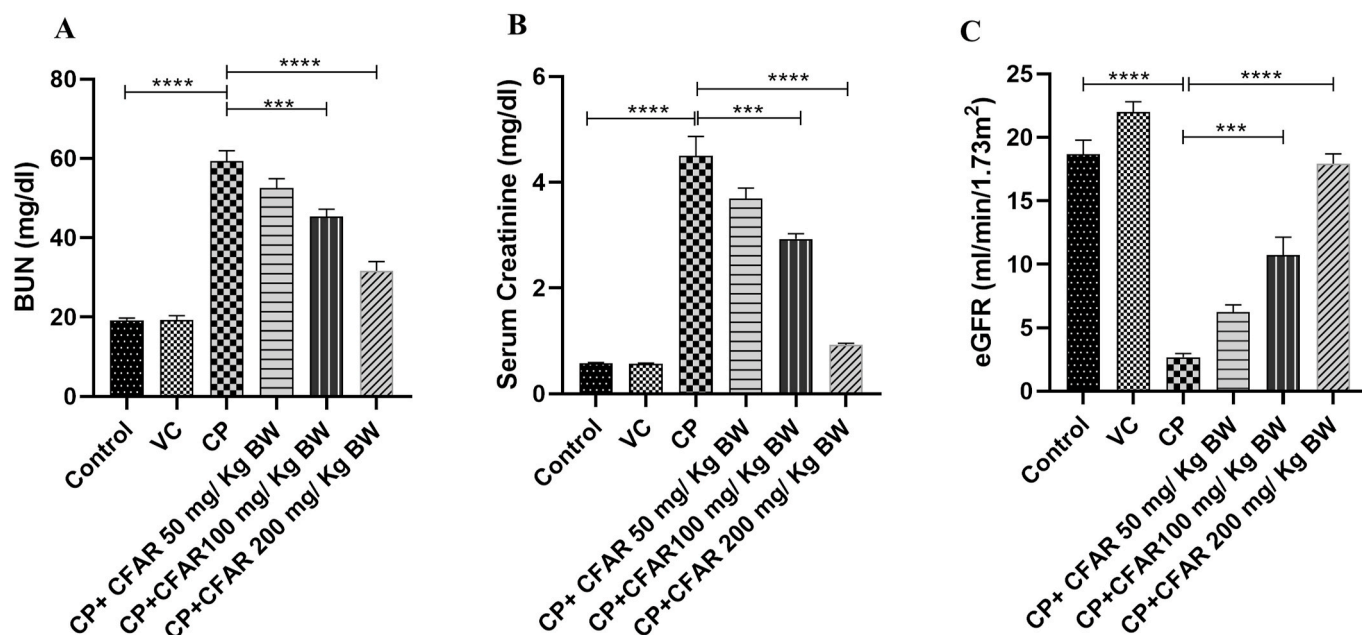


Fig. 7. Effect of CFAR on BUN (A), sCr (B) and eGFR (C) level on CP-induced AKI in rats at different dose-dependent study. The data were presented as mean \pm SE (n = 6) by two-way analysis of variance (ANOVA) followed by Tukey's multiple comparisons test, where * p < 0.05, **p < 0.01, ***p < 0.001, ****p < 0.0001.

(p < 0.05) downregulated to the CP induced group V and VI animals orally administered with the high doses (100 and 200 mg/kg bw) of CFAR as compared to group III rats. These high doses were also significantly (P < 0.05) enhanced the expression of apoptosis regulatory protein Bcl2 and Nrf2 in the kidneys tissues of group V and VI animals when compared to group III rats. These result ensures that CP-induced AKI can be prevented by the effect of phytoconstituents present in the CFAR and thereby protects the kidneys from the process of necrosis and apoptosis (Fig. 12A–G).

3.12. Effects of CFAR on histopathological changes in the kidney

Histopathological analysis of kidney tissues using H&E and PAS staining. The control and vehicle control groups showed that glomeruli and renal tubules of kidney tissues are present with well-organized histoarchitecture; there is no evidence of a lesion in the H&E stained slides. The CP-induced rats showed the loss of glomerular basement, the lumen of the renal tubules was abnormally dilated, there was the formation of many scattered hyaline casts, tubular necrosis, cellular micro debris, and loss of microvilli in tubular cells, epithelial cells were irregular and of different sizes, and there was an increased interstitial fibrosis and hypertrophy of glomeruli. Orally administration of CFAR at the doses of 100 mg and 200 mg/kg bw to the CP-induced rats, it was observed that there was very slight disorientation of the renal tubules and normal glomerulus with intact bowman's capsule. However the lower dose of CFAR at 50 mg/kg/day does not able to provide nephroprotection to the CP treated group IV animals and there was similar histological findings observed with the CP treated group III animals (Fig. 13A–F). Tubular injury scores were significantly higher in the CP treated rats, however higher doses of CFAR could able to provide the nephroprotection and thereby a significantly low tubular score was observed in group V and VI animals (Fig. 13G). In addition, PAS staining also revealed similar observation to the H&E staining, that is the structure and morphology of the glomerulus, renal tubules, and renal interstitium were normal in the control and vehicle treated groups the staining of the basement membrane indicated full integrity, and abnormal changes, such as inflammatory cell infiltration and fibrosis, were not detected. In CP-treated group III animals, the lumen of the renal tubules was abnormally dilated, the staining of the basement

membrane of tubular epithelial cells was discontinuous, epithelial cells were irregular and of different sizes, an increased interstitial fibrosis, great amount of glycogen deposition, loss of brush border and hypertrophy of glomeruli was observed. CFAR treated at 50 mg/kg bw to the CP treated group III animals, there was no alteration recorded as compared with CP treated group III animals. However CFAR at high doses (100 mg and 200 mg/kg bw) significantly ameliorated the tubular lesions and maintained minimal glycogen deposits in the basement membrane (blue arrow) with normal brush border (black arrowhead) and overall a control like histoarchitecture was observed in PAS staining (Fig. 14A–F).

4. Discussion

Herbal medicines are receiving global interest due to their remarkable biological properties, substantial economic value, and readily available supplies. Several medicinal plants and their extracts are used for the protection of kidney functions on experimental model (Meka Kedir et al., 2022). AR is among the exceptional herbal medicinal substances with remarkable properties that have been discovered. This herbal medicinal plant has demonstrated remarkable co-therapeutic effects for a variety of medical purposes, from leaves to roots. Research has demonstrated that AR possesses bioactive components such phenols, alkaloids, flavonoids, steroids, and coumarins, resveratrol and apigenin which enable it to function as adjuvant therapy and have antibacterial, anti-inflammatory, and antioxidant properties (Singh et al., 2023; Mitra et al., 2024; Aldayel, 2022). It has been discovered that HPLC works very efficiently for identifying and detecting flavonoids that are present in a variety of plants and their byproducts. Because HPLC analysis can effectively separate and sort out complicated mixtures while maintaining peak purity, it is recommended for quality control and standardization. The hydrolysis of flavonoid glycosides during the extraction process, which facilitates the detection of flavonoid aglycones, is one potential solution to this issue (Wang et al., 2016). The presence of flavonoids were identified from root of CFAR using quercetin as standard. Using quercetin as a reference, the flavonoid content of the CFAR root was determined. The CFAR employed LC-MS, a verified hyphenated and precise instrument for rapid analysis, to identify the phenolic chemicals. By comparing their retention times and mass

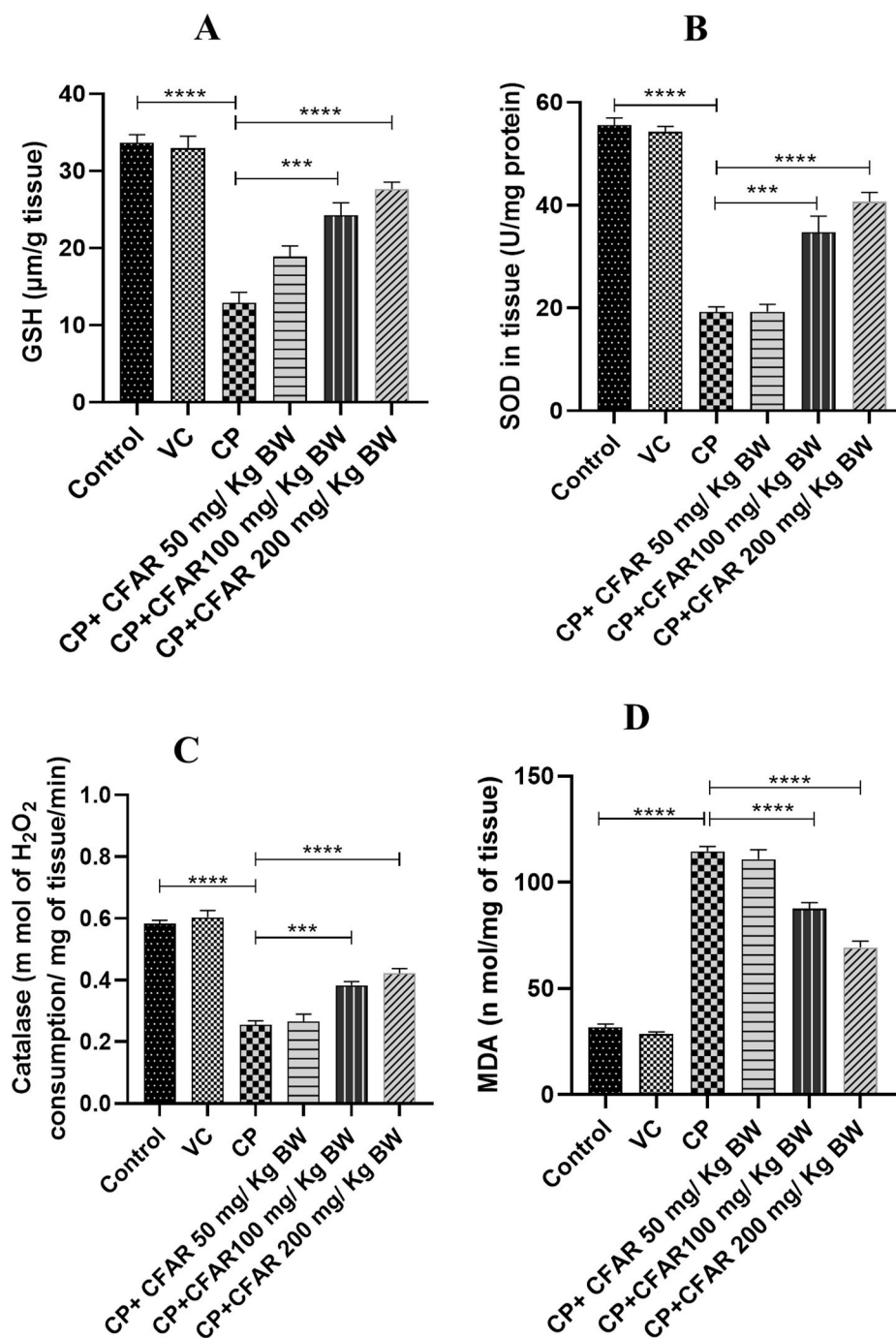


Fig. 8. The effect of CFAR on the levels of enzymatic and non-enzymatic antioxidant parameters of CP-induced AKI in rats. GSH (A), SOD (B), CAT (C) and MDA (D); Data were presented as mean \pm SE (n = 6) by two-way analysis of variance (ANOVA) followed by Tukey's multiple comparisons test, where * p < 0.05, **p < 0.01, ***p < 0.001, ****p < 0.0001.

fragmentation pattern, bioactive compounds such as 4-Oxo-L-isoleucine, flavone, D-pantothenic acid, syringic acid, orientin, bianthrone, cathine, apigenin, resveratrol, azafirin, isoarborinol, curcumin, β -sitosterol, etc. were identified from the LCMS analysis run in both positive and negative ionization mode (Table 2). The CFAR may include these phytochemicals, which have the potential to offer nephroprotective benefits against CP-induced AKI. It was reported that isolated plant based bioactive compounds like apigenin and resveratrol have protected streptozotocin induced diabetic nephropathy as well as end stage renal diseases due to their anti-oxidative and anti-inflammation activities (Mitra et al., 2024).

Cytotoxicity by MTT assays is a sensitive and comprehensive method

to evaluate the integrity of cells against medications and chemicals (Ghasemi et al., 2021). Cisplatin led to a significant increase in cell death with changes in normal cellular morphology in NRK-52E cells. NRK-52E cells treated with CP and CFAR resulted in significant enhancement of cell growth compared to CP treated group indicating the cytoprotective activity of CFAR against CP-induced cytotoxicity. Our results exhibited the protective role of CFAR in retaining the viability of NRK-52E cells administered with CP, representing the AKI model.

Cells treated with CP showed impaired membrane integrity and nucleus were stained with EtBr, whereas membranes of dead or alive cells are stained with the vital dye AO. As a consequence, normal undamaged cells seem green, while cells in early or late stages of apoptosis

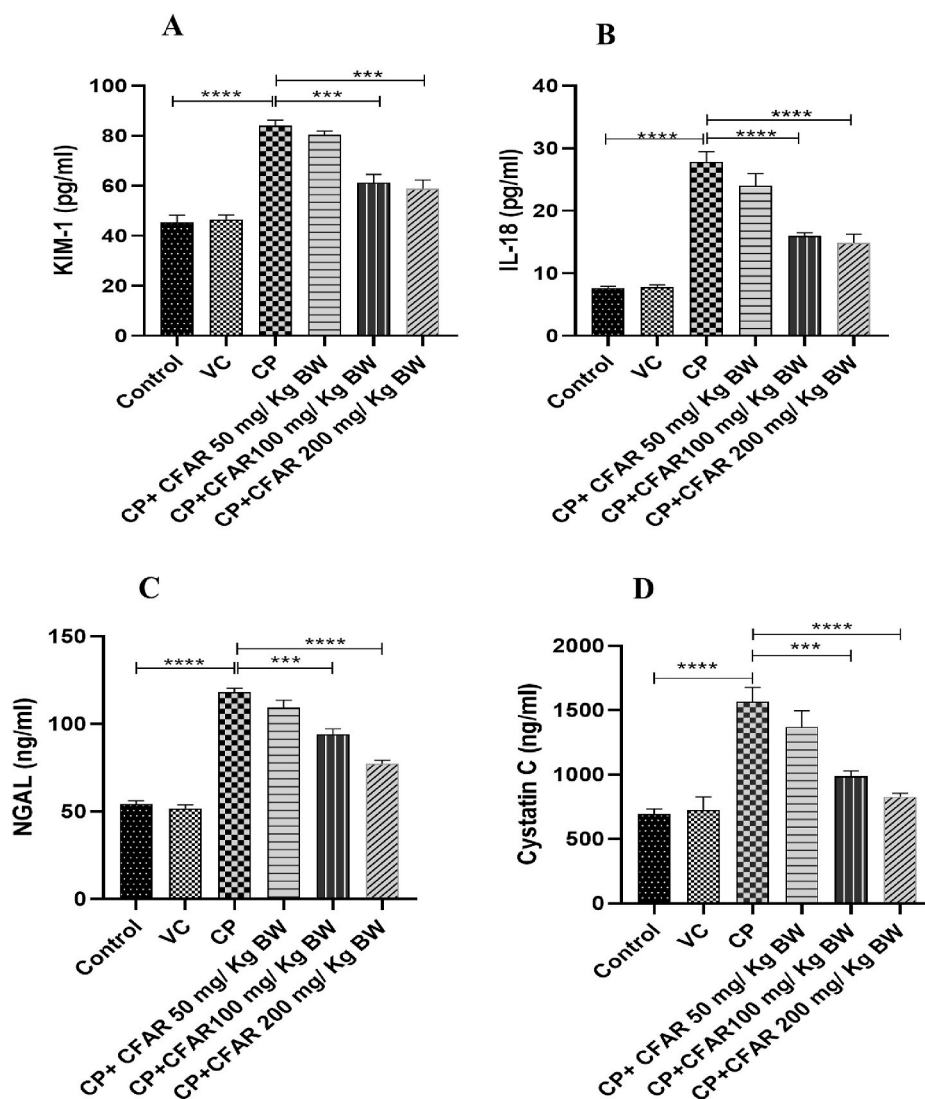


Fig. 9. Effect of CFAR on urinary KIM 1 (A), IL-18 (B), NGAL (C), and Cys C (D) levels in CP induced rats. This data were generated as mean \pm SE (n = 6) by two-way analysis of variance (ANOVA) followed by Tukey's multiple comparisons test, where * p < 0.05, **p < 0.01, ***p < 0.001, ****p < 0.0001.

with condensed and shattered nuclei look reddish-orange and yellowish-orange, respectively. In contrast, necrotic cells will colour orange even if they lack condensed chromatin and have normal nuclear morphology, when viewed under a fluorescence microscope. NRK-52E cells going through apoptosis show condensed chromatin and AO/EB dual staining, whereas living, healthy cells appear green (only AO staining) (Guo et al., 2012). Our result reported that different doses of CFAR (50 μ g–400 μ g) could reduce CP-induced cell death and apoptosis by maintaining a control like cell morphology.

Cisplatin-induced anorexia has been shown to be mediated by reductions in serotonin secretion from enterochromaffin cells and plasma ghrelin level. These actions both lessen the urge to eat and the body's ability to utilize the food that is consumed efficiently, which results in weight loss and an increase in renal somatic index. Additionally, the elevation of other renal biomarkers and kidney enlargement support the pathophysiological edema that causes rhabdomyolysis after toxin exposure (Takeda et al., 2008; Lin et al., 2018). Interestingly, in the AKI intervention paradigm, natural plant metabolic compounds not only prevented body weight loss but also enhanced food intake by inducing hormones (Lin et al., 2018). The results of the current investigation showed that CFAR roots, at doses of 100 and 200 mg/kg body weight on CP-induced AKI, contain a large number of bioactive secondary metabolites that may assist maintaining normal body weight and renal

somatic index. Renal injury brought on by cytotoxic drugs like CP is caused by a number of mechanisms, including tubular cell death, tissue destruction from inflammatory cytokine releasing, and a vicious cycle of oxidative stress and inflammatory reactions (Oh et al., 2014). The waste products of metabolism, BUN and sCr, are eliminated by the kidneys through the urine. Urea and creatinine pass from blood to the glomerular filtrate the liquid that serves as the starting point for urine during the process of glomerular filtration. The amount of urea that enters the proximal tube of the nephron from the glomerulus is determined by the GFR because the concentration of urea in the filtrate as it forms is identical to that in plasma (Udupa and Prakash, 2018). Increased glomerular capillary hydraulic pressure can result in a progressive decline in GFR and end-stage renal disease. It can also be caused by changes in efferent and afferent arteriolar resistances and/or systemic arterial pressure (Palatini, 2012). Plant-based flavonoids are useful in lowering glomerular hypertension and slowing the decline of renal function because they work on the renin-angiotensin-aldosterone pathway (Alshahrani, 2023; Cao et al., 2022; Meghji et al., 2019). Phytocompounds have the potential to enhance tubular function and avoid several renal problems, including drug-induced renal damage, ischemia-reperfusion injury, and sepsis-induced renal injury (Bilgiç et al., 2017; Hao et al., 2016). AKI may result from the intramuscular injection of a nephrotoxic component that induces rhabdomyolysis. The

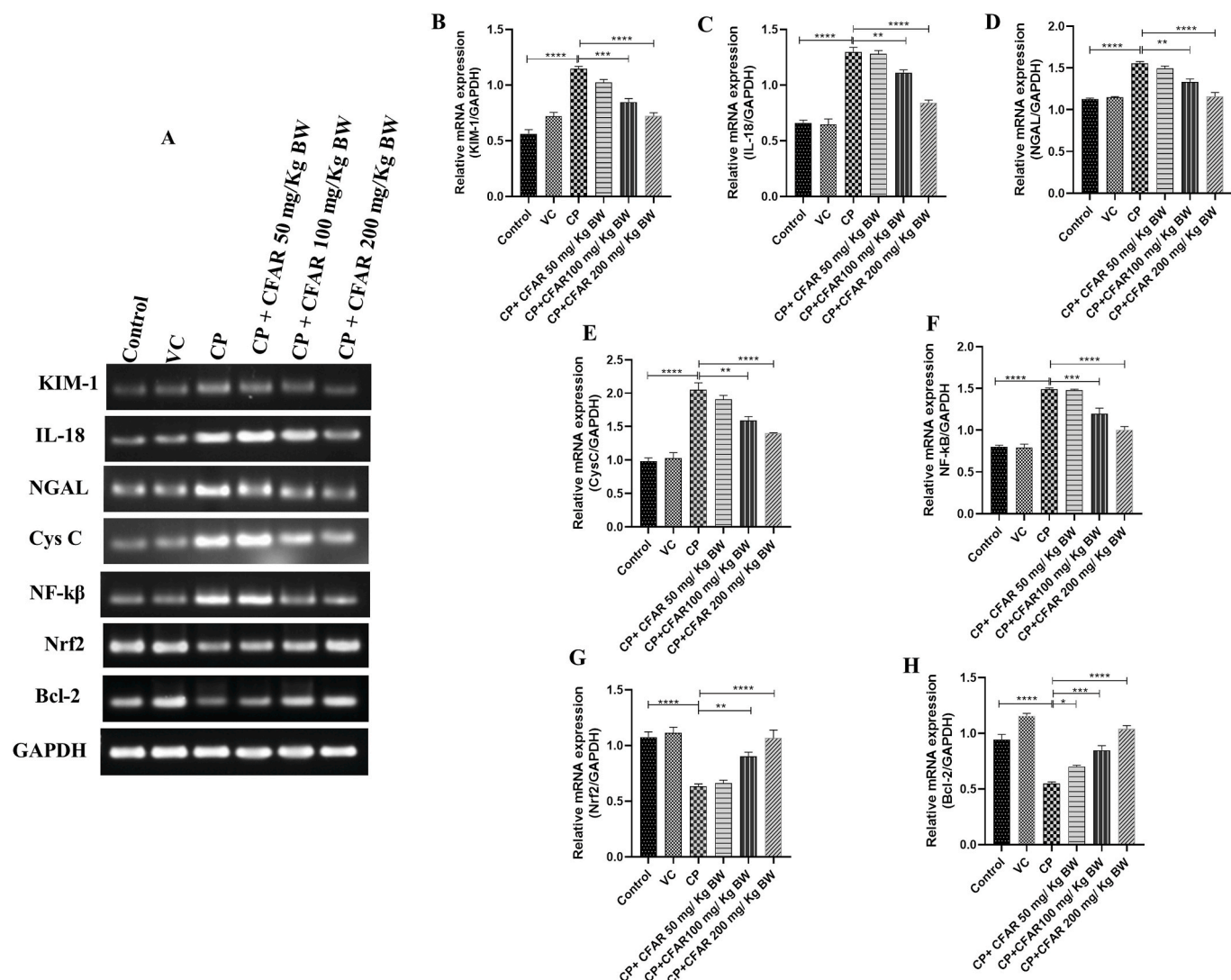


Fig. 10. Effect of CFAR on the relative mRNA expression by semi qPCR (A) for KIM1 (B), IL-18 (C), NGAL (D), Cys C (E), NF-k β (F), Nrf2 (G) and Bcl2 (H) on CP induced AKI. The values were plotted from the densitometric analysis by ImageJ software and then data were presented as mean \pm SE (n = 6) by two-way analysis of variance (ANOVA) followed by Tukey's multiple comparisons test, where * p < 0.05, ** p < 0.01, *** p < 0.001, **** p < 0.0001.

renal tubule becomes clogged with this debris when skeletal muscles released their contents into the bloodstream. The primary end point was defined as an absolute rise in the baseline sCr and BUN levels following a 24-h drugs injection (Rizk et al., 2023). Treatment of animals with apigenin prior to drug including CP and gentamicin injection showed marked decrease in serum levels of creatinine and BUN, indicating improvement of kidney functions (Hassan et al., 2017; Hussein et al., 2022). In this study CP causes AKI and thereby level of functional markers like sCr and BUN level was increased to very high level. After administration of CFAR at the high doses, it was found that there was decreased production of BUN and sCr and also improved eGFR functionality that indicate the compounds presents in this fraction of AR roots can protect renal cells to survive and prevent development of AKI.

Oxidative stress is a major factor in the development of nephron injury or death (Kong et al., 2020). Changes in both enzymatic and non-enzymatic antioxidants and increased ROS reaction on cellular biological macromolecules on the biofilm led to the production of lipid peroxidation products, including MDA. Oxygen free radicals cause cellular damage and elevate the level of MDA. After then, a lot of antioxidant enzymes, such as SOD and GSH, were used to get rid of extra free radicals (Xue et al., 2023). Acute oxidative damage was demonstrated in

this work by enhanced ROS production and lipid peroxidation through the generation of MDA levels as a result of AKI induction, whereas the antioxidant markers (CAT), GSH, and SOD were decreased. When CFAR was fed orally, redox alterations in the AKI model were observed, as evidenced by a decrease in MDA and a rise in (CAT), SOD, and GSH levels in contrast to the CP-induced AKI model. Our findings shown that AR root, which has the highest ROS scavenging action on CP-induced AKI, can be utilized as an efficient natural source of polyphenols and antioxidants. Additionally, it is abundantly clear from the literature that bioactive compounds exhibit their antioxidant action by preventing the generation of ROS as a result of Nrf2 activation (Hassanein et al., 2019). Cisplatin nephrotoxicity is related to free radical generation and the nephroprotection offered by bioactive compound like apigenin is due to their antioxidant defense system. Additionally, it is abundantly clear that apigenin and resveratrol, revealed that drug caused a severe reduction in SOD activity and GSH levels, accompanied by an increase in MDA, leading to the overproduction of ROS and induction of oxidative injuries. Noteworthy, these changes were suppressed by apigenin, consistent with several previous reports (Kara et al., 2022; Wu et al., 2021; Hassan et al., 2017). There is evidence to support Nrf2 function in protecting the kidneys from a variety of illnesses, including drug-induced renal injury. Additionally, Nrf2 has anti-inflammatory

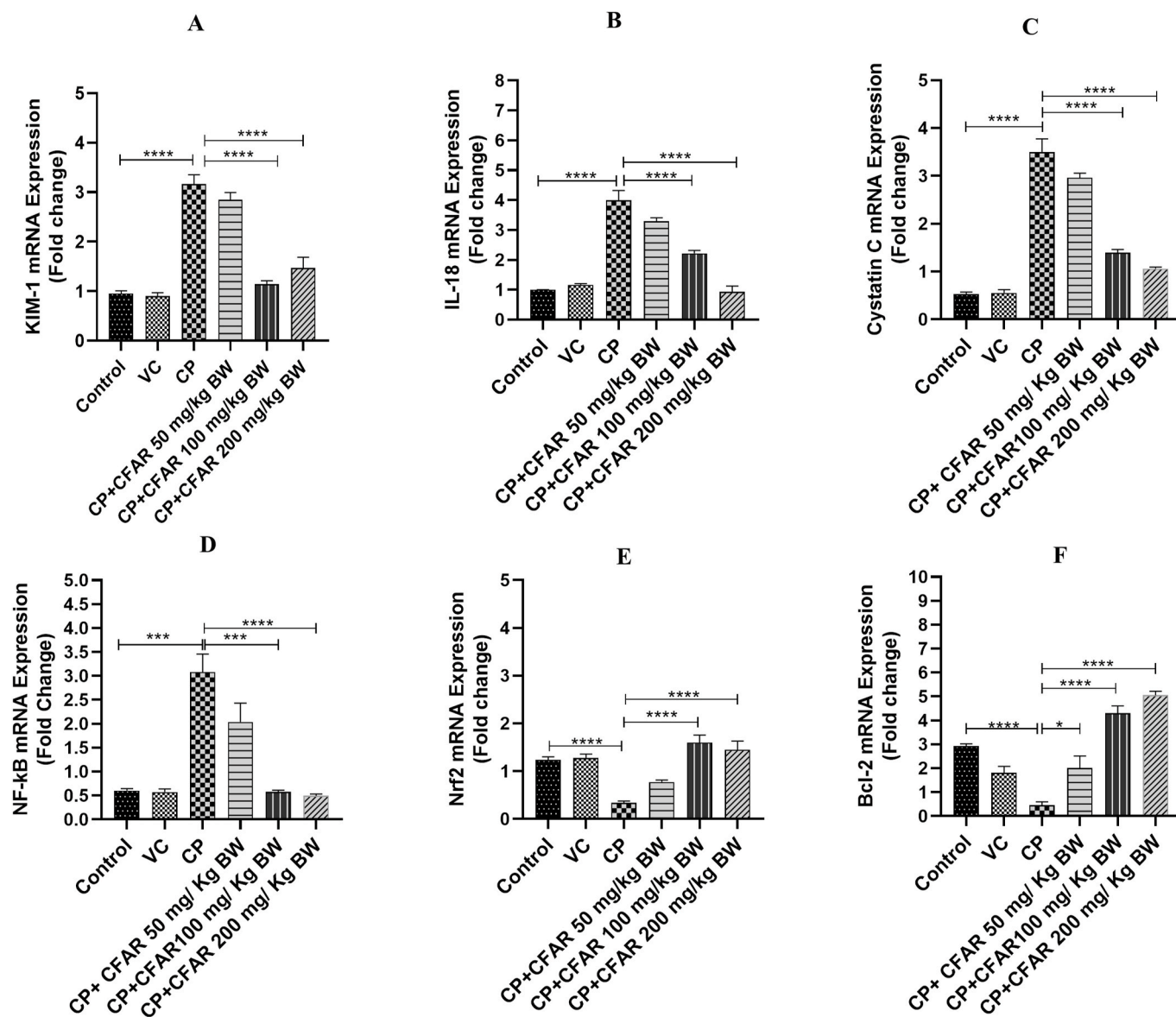


Fig. 11. Effect of CFAR on relative mRNA expression of KIM-1 (A), IL-18 (B), Cys C (C), NF-kB (D), Nrf2 (E) and Bcl2 (F) in kidney tissues against CP-induced AKI in rats by qRT-PCR. GAPDH was used for normalized of relative gene expression. Data were presented the fold changes in the relative mRNA expression as Mean \pm SE (n = 6), by two-way analysis of variance (ANOVA) followed by Tukey's multiple comparisons test, where * p < 0.05, **p < 0.01, ***p < 0.001, ****p < 0.0001.

qualities that make it a useful marker for determining how well any therapeutic substance responds for managing AKI caused by drugs. The removal of toxins and ROS is one of Nrf2 activation's cytoprotective effects, and these processes are probably crucial in nephrotoxicity. According to certain tests, Nrf2 activation plays a role in Bcl-2 activation, which controls cellular survival and apoptosis. Together with a host of cytoprotective genes that encode detoxification enzymes, antioxidant proteins, and drug transporters, Nrf2 also up-regulates the expression of the Bcl-2 gene. Consequently, it makes sense to conclude that the coordinated activation of Bcl-2, an anti-apoptotic protein, and cytoprotective proteins decreased apoptosis and increased cell survival (Niture and Jaiswal, 2012; Li et al., 2018; Ortega-Domínguez et al., 2017; McSweeney et al., 2021; Ma et al., 2019). The interaction of Bcl-2 family members can cause mitochondrial damage by triggering the outer membrane permeabilization and loss of mitochondrial membrane potential. The release of cytochrome C from mitochondria into the cytosol and the activation of the caspase cascade in the mitochondrial pathway can result from a breakdown of the potential of the mitochondrial membrane. According to an insilico study, phytochemicals have strong

antioxidative potential because they modulate the binding of the Nrf2/Bcl2 gene and downregulate the release of cytochrome C, which controls the cell's natural antioxidant defense mechanism (Molaei et al., 2021; Hassanein et al., 2019). Moreover, apigenin administration suppressed renal inflammation and apoptosis by decreasing levels of NFkB, while increasing Bcl2 compared with those in gentamicin-administered group (Hussein et al., 2022) and ischemia/reperfusion injury (He et al., 2021). Apigenin also attenuates renal tubular damage by increasing the mRNA levels of Nrf2 and subsequently increasing the antioxidant enzymes (Aldayel, 2022). In the present investigation, the CP-treated group exhibited a considerable down-regulation of Nrf2/Bcl2 expression in contrast to the normal control group. On the other hand, bioactive compounds like resveratrol in CFAR can trigger upregulation of Nrf2/Bcl2 expression both in kidney tissue protein and mRNA. Study reported that resveratrol not only scavenges ROS but also, through transcriptional control via Nrf2, regulates the production and activity of antioxidant enzymes, including CAT, GSH and SOD (Kitada and Koya, 2013). So, the potent antioxidant activity of CFAR exerts through modulation of Nrf2/Bcl2 that regulates endogenous antioxidant defense

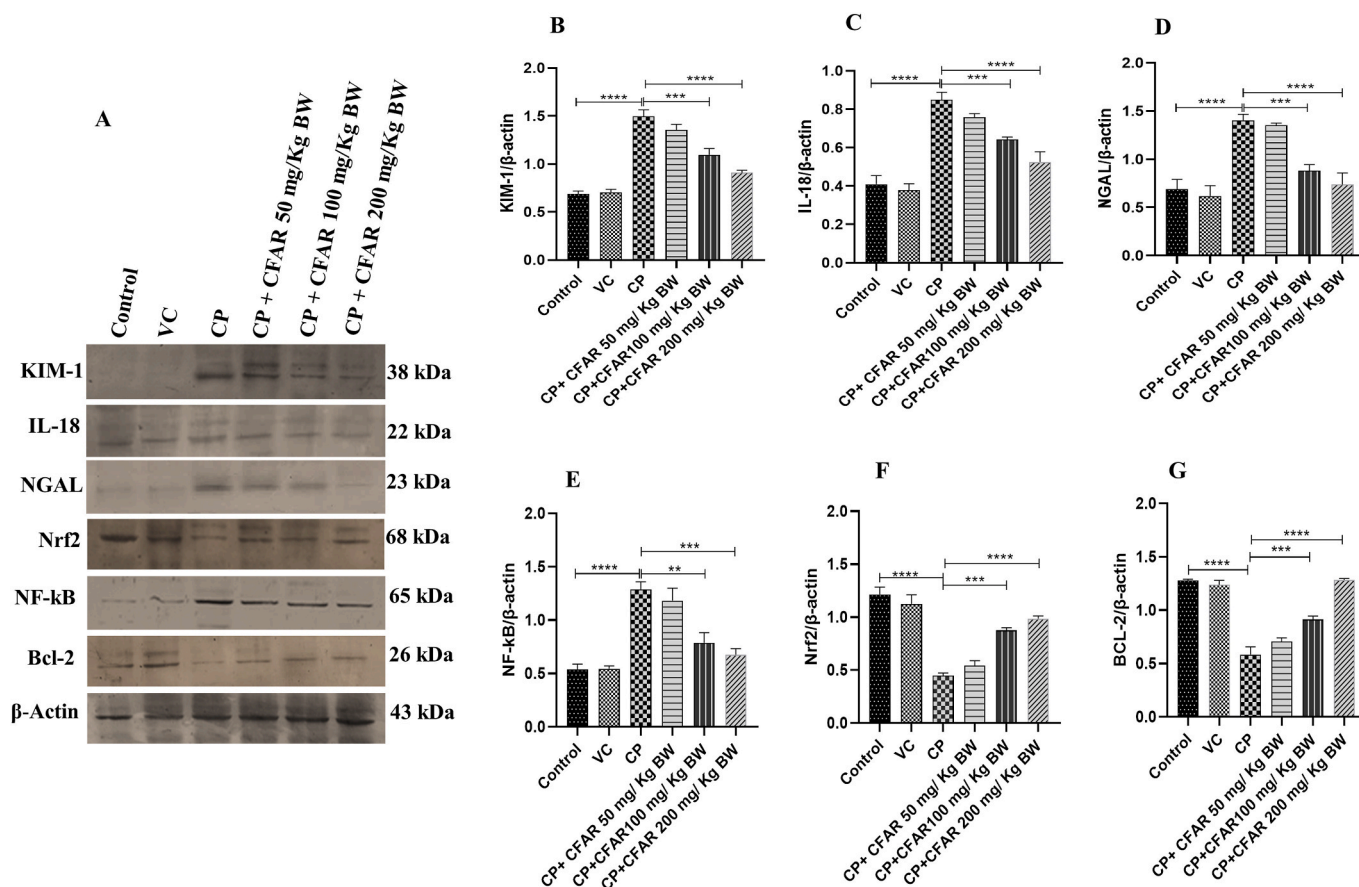


Fig. 12. Effect of CFAR on the protein expression level of CP induced AKI by immunoblotting (A). Inflammatory markers of specific protein expression level of KIM-1 (B), IL-18 (C), NGAL (D) and the expression level of apoptotic marker NF-KB (E), Nrf2 (F), Bcl-2 (G), in kidney tissues. Densitometric analysis was expressed as mean \pm SE (n = 6) by two-way analysis of variance (ANOVA) followed by Tukey's multiple comparisons test, where * p < 0.05, **p < 0.01, ***p < 0.001, ****p < 0.0001.

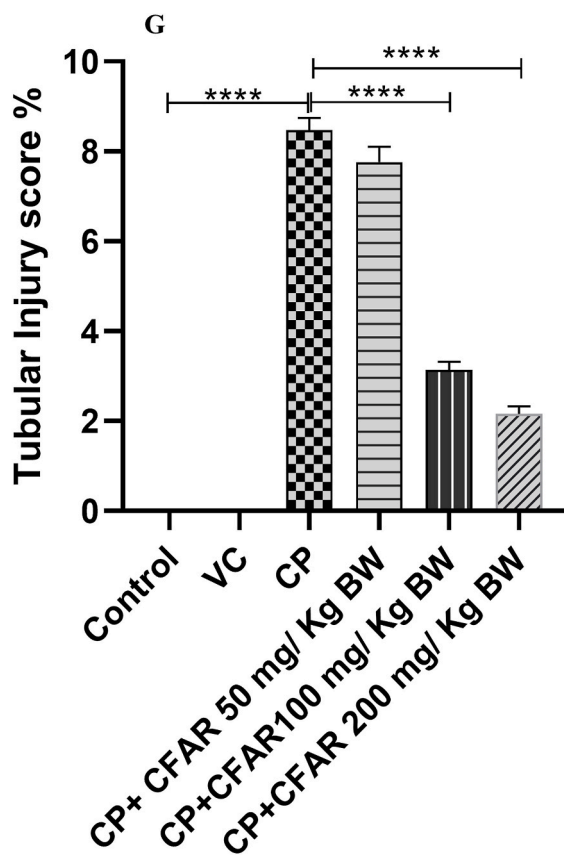
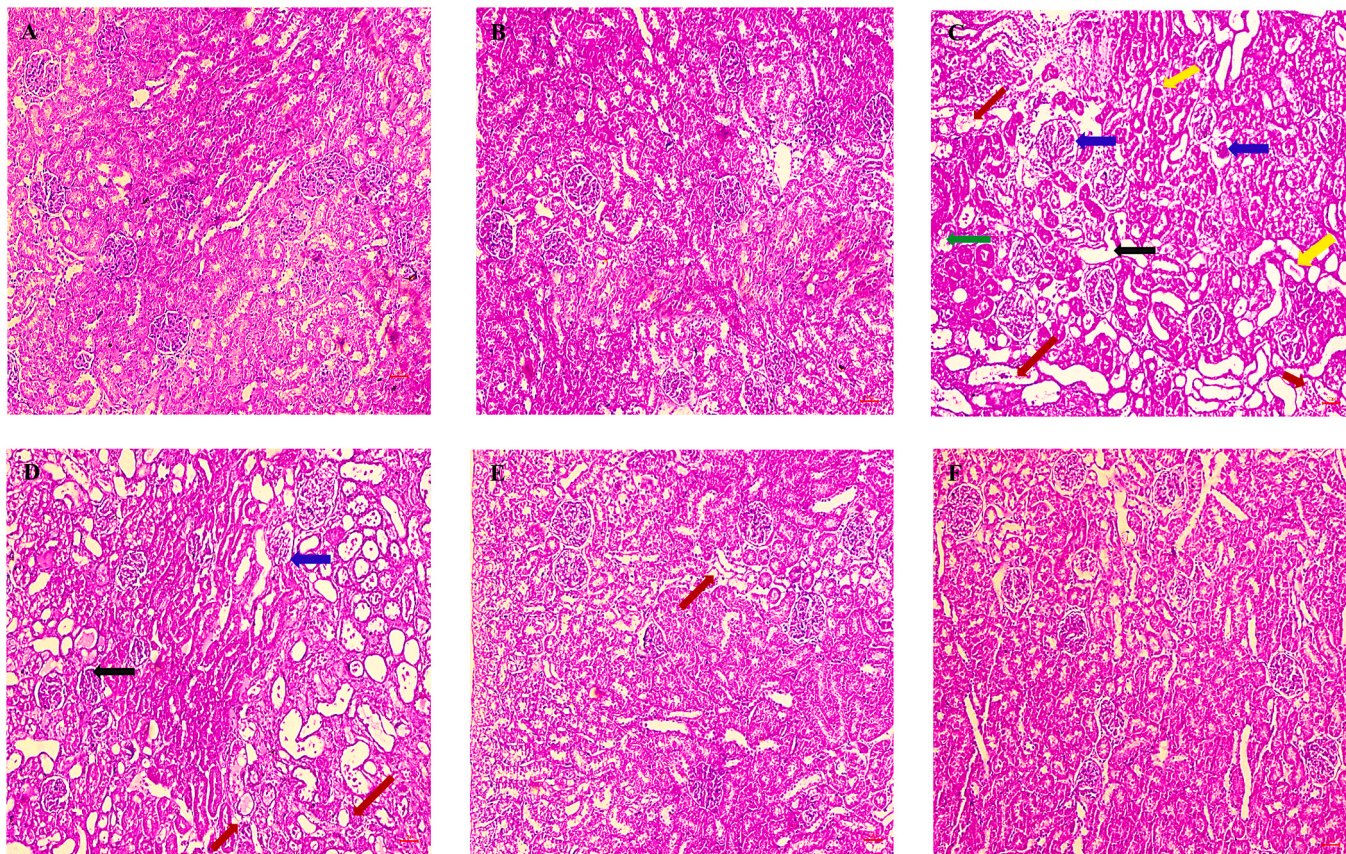
system on CP-induced AKI.

Numerous investigations have shown that when tubular damage occurs, NGAL and KIM-1, a renal injury biomarker, are released instantly. NGAL is largely up-regulated within thick ascending limb of henle's loop, according to gene expression studies in AKI. The majority of urinary NGAL appears to be secreted into the urine by the distal tubules, which is likely more indicative of a traditional marker of kidney injury (Schmidt-Ott et al., 2007; Han et al., 2009). In other words, the mRNA and protein expression of NGAL and KIM-1 was significantly upregulated in unilateral ureteric obstruction and CP-induced *in vivo* model for evaluating renal tubular damage and inflammation. The relative levels of NGAL and KIM-1 in patients with AKI correlate with the severity of the risk of mortality (Xu et al., 2021). However, because of the pharmacological actions of the plant, plant extracts can prevent drug-induced various biomarkers by inhibiting the receptor site of the inflammatory condition in the renal tissues of the AKI model (Rizk et al., 2023). According to our findings, rats given high doses of CFAR had significant modulation of their KIM-1 and NGAL levels, and these biomarkers' levels returned to normal. This demonstrates that the CFAR's chemical constituents may support both its protective function in averting renal cell damage and its nephroprotective qualities. The fraction derived from the AR root contains a number of phytomolecules that have been demonstrated to be beneficial in preventing kidney damage by lowering other biomarkers, such as Cys C, which is completely reabsorbed in the proximal tubule after being filtered by the renal glomeruli and may be a valuable marker for AKI. This is in line with earlier research examining the impact of plant extracts or chemicals on Cys C (Ali et al., 2022; Bayrak et al., 2008; Hussein et al., 2022).

Drugs have the ability to release cytokines linked to inflammation,

such as IL-18. This is achieved by ligand binding to the receptor complex, which releases NF- κ B and translocates it to the nucleus where it is used for gene transcription (Elsherbiny and Al-Gayyar, 2016). In rats, an increase in kidney NF- κ B expression 24–48 h after drug administration was found to be engaged in tandem with the development of AKI (Korrapati et al., 2012). Although NF- κ B is a strong inflammatory mediator, it also stimulates inflammatory factors like IL-18 and is essential for the production of pro-inflammatory cytokines. IL-18 permits the early diagnosis of kidney injury caused by ischemia or nephrotoxicity. Furthermore, gene polymorphism of pro-inflammatory cytokines and their receptors can be used as a powerful predictor of the susceptibility and progression of nephropathy due to altered translational/post-translational mechanisms (Al Asmari et al., 2017). Flavonoids can prevent renal dysfunction and improve renal function by blocking or suppressing of mRNA and protein expression of NF- κ B and IL-18 (Kumar et al., 2015). The early diagnosis of kidney injury caused by ischemia or nephrotoxicity is made possible by IL-18. The findings of this study unequivocally indicate that CFAR include a large number of bioactive phytocompounds that aid in reducing the expression of inflammatory markers such as IL-18 and NF- κ B in order to prevent renal inflammation.

A decrease in the number of cells in the glomeruli, a loss of cellular tubular constituents, vascular congestion leading to epithelial cell atrophy, deformations of the epithelial membrane of the bowman capsule, and deformation of the bowman space are among the abnormal changes in the kidney tissue that have been found to occur when toxic drugs are present. Polyphenols and flavonoids have been shown to improve the architecture of kidney tissue by reducing the nephrotoxicity of drugs; this could be a mechanism for the epithelial–mesenchymal transition



(caption on next page)

Fig. 13. H&E staining of rats kidney tissue sections of the experimental animals under 10X. Control and vehicle control groups (A, B) showed normal and organized histoarchitecture of kidney tissue with intact glomerulus and renal tubules properly arranged. In cisplatin treated group (C) the tubular lumen was enlarged and dilated (black arrow); formation of hyaline cast (yellow arrow), tubular necrosis (red arrow), hypertrophy glomerular (blue arrow) and cellular micro debris (green arrow) in tubular cells were observed. CFAR administered at 50 mg/kg bw to the CP treated group (D) revealed necrosis of many renal tubules (black arrow) with the presence of hyaline casts (red arrow). CFAR at high doses (100 mg, 200 mg/kg bw) along with CP administration to the rats (E, F), there was significantly less tubular lesions and maintained a control like histoarchitecture of the kidney tissue section. Only a slight disorientation (red arrow) was observed in the tubular part. AKI rats administered with high doses of CFAR showed significantly lower tubular injury score (G) compared to the CP treated AKI group. For control and vehicle control group the tissue sections of rat kidney tissues were observed with normal histoarchitecture and thereby no evident tubular score was observed. Data were expressed as Mean \pm SE (n = 6) by two-way analysis of variance (ANOVA) followed by Tukey's multiple comparisons test, where * p < 0.05, **p < 0.01, ***p < 0.001, ****p < 0.0001. (For interpretation of the references to colour in this figure legend, the reader is referred to the Web version of this article.)

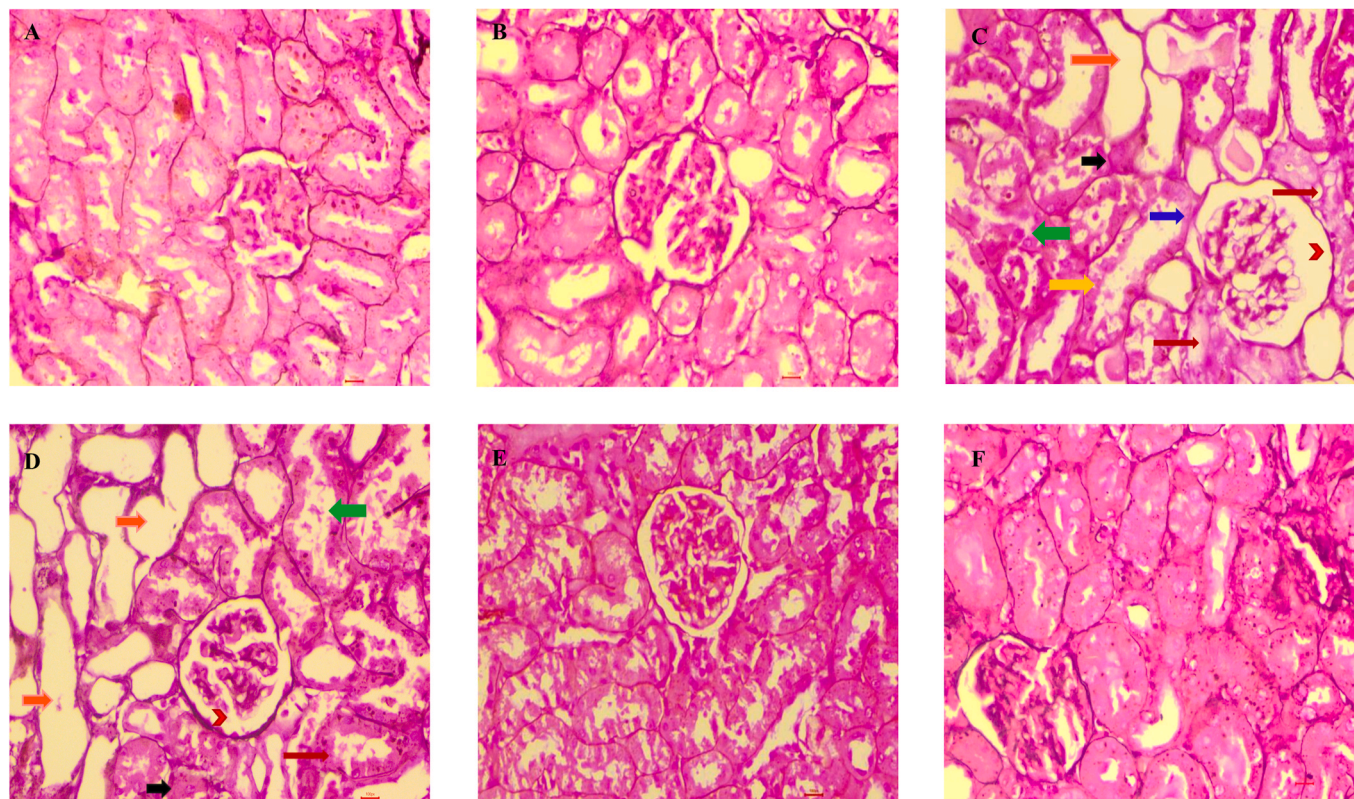


Fig. 14. PAS staining of rats kidney tissue sections of the experimental animals under 40X. PAS staining demonstrated that the structure and morphology of the glomerulus, renal tubules, and renal interstitium were normal in the control and vehicle treated group (A,B); the staining of the basement membrane indicated full integrity, and abnormal changes, such as inflammatory cell infiltration and fibrosis, were not detected. In the cisplatin treated group (C), the lumen of the renal tubules was abnormally dilated (orange arrow); the staining of the basement membrane of tubular epithelial cells was discontinuous (green arrow), and epithelial cells were irregular and of different sizes (yellow arrow), an increased interstitial fibrosis (red arrow), great amount of glycogen deposition (black arrow) and loss of brush border glycogen deposition (blue arrow), also noted the hypertrophy of glomeruli (red arrowhead). CFAR treated at 50 mg/kg bw with CP group (D), there was no alteration observed as compared with CP treated AKI group. High doses of CFAR (100 mg, 200 mg/kg bw) administration to the CP-induced rats (E, F), there was no evident tubular lesions observed and a well maintained histoarchitecture with intact glomerulus was found. (For interpretation of the references to colour in this figure legend, the reader is referred to the Web version of this article.)

(EMT), a process that enables stressed tubular cells to become mesenchymal with an increased capacity to produce extracellular matrix (ECM) (Kalluri and Weinberg, 2009; Bencheikh et al., 2021). According to a study, the kidney of rats given CP and resveratrol at the same time displayed cortex with a normal glomerulus. According to these findings, when CP was treated with resveratrol concurrently, the nuclei seemed euchromatic, the apical microvilli were ordered, and the mitochondria and intervals between the cytoplasmic infolding appeared normal (Osman et al., 2015). Glycogen deposition has been linked to tubular cells' ability to adapt to adverse conditions. In this investigation, CP-treated AKI rats displayed extracellular matrix deposition, tubular dilatation, inflammatory cell infiltration, atrophy, and degenerative changes of the tubular epithelium. Conversely, when CFAR roots were taken orally in large doses, no specific harm was observed and the histoarchitecture of the renal tissues was preserved with a normal renal

tubular morphology and typical glomeruli.

5. Conclusion

In summary, this study has produced evidence from science to back up the use of AR to slow the onset of AKI. Due to these benefits, AR can prevent AKI from progressing to ESRD and these effects may be attributed to the bioactive phytochemicals in AR, which have a renal protective impact by blocking the NF κ B/IL-18 signaling pathway and perhaps boosting the expression of Nrf2/Bcl2 (Fig. 15). The primary causes of its pharmacological effectiveness are its anti-oxidant and anti-inflammatory properties. Further research is necessary to fully understand each compound's efficacy. These results thus support the notion that this medicinal plant helps to safeguard kidney functions and open the door for its potential application as an AKI treatment agent.

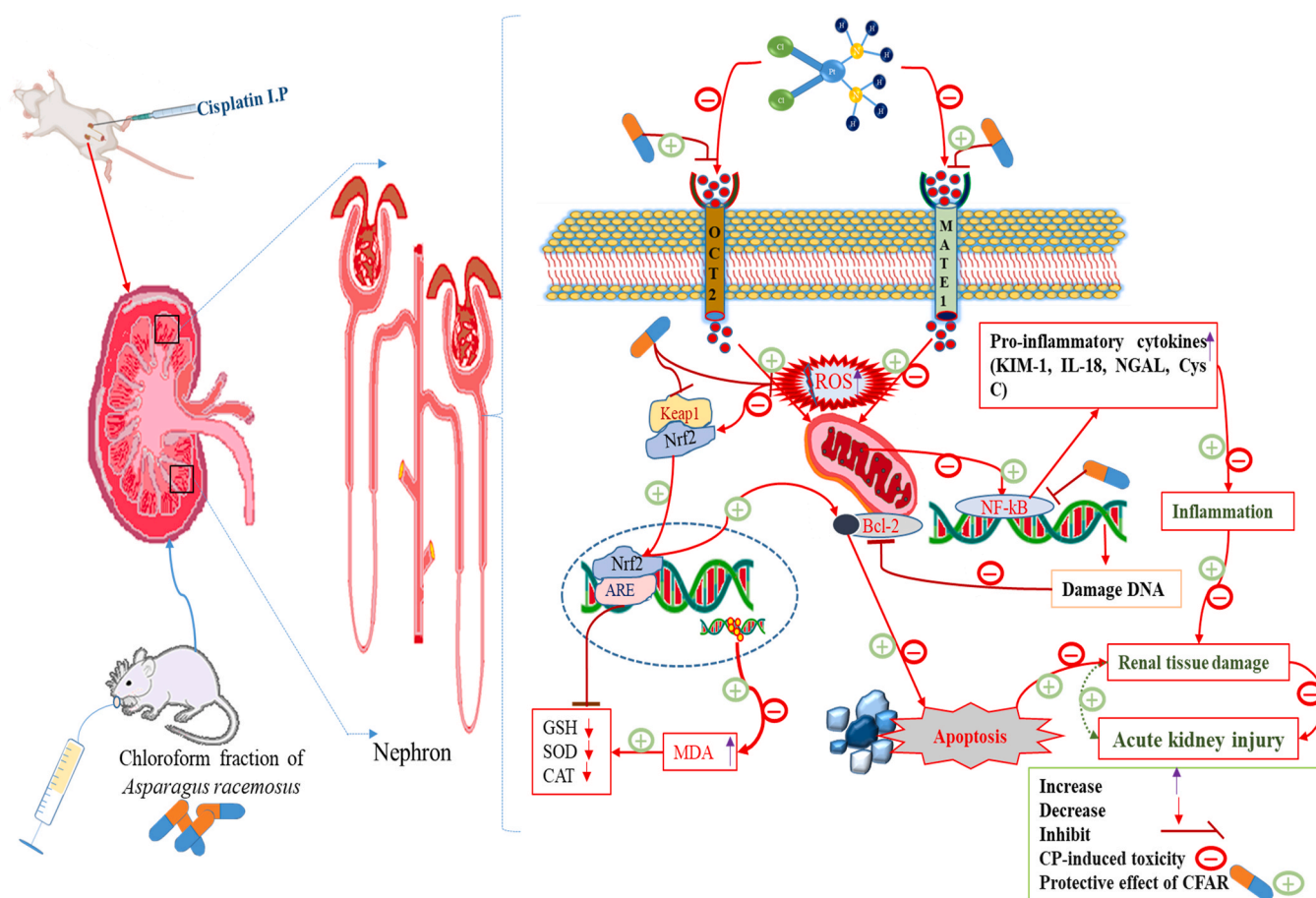


Fig. 15. The possible and hypothetical mechanism of nephroprotective properties of CFAR on CP-induced AKI.

CRedit authorship contribution statement

Sahadeb Jana: Writing – original draft, Resources, Methodology, Formal analysis, Data curation. **Palash Mitra:** Software, Resources, Methodology, Investigation. **Titli Panchali:** Methodology, Investigation, Data curation. **Amina Khatun:** Methodology, Investigation, Data curation. **Tridip Kumar Das:** Methodology, Investigation, Formal analysis, Data curation. **Kuntal Ghosh:** Writing – review & editing, Validation, Supervision. **Shrabani Pradhan:** Writing – review & editing, Validation, Supervision. **Sudipta Chakrabarti:** Writing – review & editing, Validation, Supervision. **Suchismita Roy:** Writing – review & editing, Visualization, Validation, Supervision, Resources, Project administration, Investigation, Funding acquisition, Formal analysis, Conceptualization.

Declaration of competing interest

The authors declare that they have no known competing financial interests or personal relationships that could have appeared to influence the work reported in this paper.

Acknowledgements

This work was supported by the Indian Council of Medical Research (ICMR), Govt. of India for providing fund under Extramural research Grant with reference no- 5/4/7-15/Nephro/2021-NCD-II, dated 3 August 2021. The authors grateful to Dr. Pradip Ghosh, Director, Midnapore City College for essential support, a well-organized work environment and laboratory facilities for conducting related research work.

Abbreviation

AKI	Acute kidney injury
AR	<i>Asparagus racemosus</i>
ARE	Antioxidant responsive element
AO/EB	Acridine orange and ethidium bromide staining
Bcl2	B-cell leukemia
BUN	Blood urea nitrogen
BW	Body weight
CFAR	Chloroform fraction of <i>Asparagus racemosus</i>
CP	Cisplatin
Cys-C	Cystatin C
ECM	Extracellular matrix
eGFR	Estimated glomerular filtration rate
EMT	Epithelial–mesenchymal transition
ESRD	End stage renal disease
GSH	Glutathione
H & E	Hematoxylin and eosin
HPLC	High performance liquid chromatography
IL-18	Interleukin-18
KIM-1	Kidney injury molecules
MDA	Malondialdehyde
NF-kB	Nuclear factor kappa-light-chain-enhancer of activated B cells
NGAL	Neutrophil gelatinase associated lipocalin
Nrf2	Nuclear factor erythroid 2-related factor 2
NRK-52E	Normal rat kidney
PAS	Periodic acid-Schiff
PBS	Phosphate buffer saline
RIPA	Radio immunoprecipitation assay
sCr	Serum creatinine

SOD Superoxide dismutase
VC Vehicle control

Data availability

Data will be made available on request.

References

- Akhtar, S., Gupta, A.K., Naik, B., Kumar, V., Ranjan, R., Jha, A.K., 2024. Exploring pharmacological properties and food applications of *Asparagus racemosus* (Shatavari). *Food Chem. Adv.* 4, 100689.
- Al Asmari, A.K., Al Sadoon, K.T., Obaid, A.A., Yesunayagam, D., Tariq, M., 2017. Protective effect of quinacrine against glycerol-induced acute kidney injury in rats. *BMC Nephrol.* 18 (1), 41. <https://doi.org/10.1186/s12882-017-0450-8>.
- Aldayel, T.S., 2022. Apigenin attenuates high-fat diet-induced nephropathy in rats by hypoglycemic and hypolipidemic effects, and concomitant activation of the Nrf2/antioxidant axis. *J. Funct. Foods* 99, 105295.
- Ali, A., Lima Sampaio, T., Khan, H., Jeandet, P., Küpeli Akkol, E., Bahadar, H., et al., 2022. Plants with therapeutic potential for ischemic acute kidney injury: a systematic review. *Evid. Based Complement Alternat. Med.* 2022, 6807700. <https://doi.org/10.1155/2022/6807700>.
- Alok, S., Jain, S.K., Verma, A., Kumar, M., Mahor, A., Sabharwal, M., 2013. Plant profile, phytochemistry and pharmacology of *Asparagus racemosus* (Shatavari): a review. *Asian Pacif. J. Trop. Dis.* 3 (3), 242–251. [https://doi.org/10.1016/S2222-1808\(13\)60049-3](https://doi.org/10.1016/S2222-1808(13)60049-3).
- Alorabi, M., Cavalu, S., Al-Kuraishy, H.M., Al-Gareeb, A.I., Mostafa-Hedeab, G., Negm, W.A., et al., 2022. Pentoxifylline and berberine mitigate diclofenac-induced acute nephrotoxicity in male rats via modulation of inflammation and oxidative stress. *Biomed. Pharmacother.* 152, 113225. <https://doi.org/10.1016/j.biopha.2022.113225>.
- Alshahrani, S., 2023. Renin-angiotensin-aldosterone pathway modulators in chronic kidney disease: a comparative review. *Front. Pharmacol.* 14, 1101068. <https://doi.org/10.3389/fphar.2023.1101068>.
- Ambavade, S.D., Misar, A.V., Ambavade, P.D., 2014. Pharmacological, nutritional, and analytical aspects of β -sitosterol: a review. *Orien. Pharma. Ex.Med.* 14, 193–211. <https://doi.org/10.1007/s13596-014-0151-9>.
- Atessahin, A., Yilmaz, S., Karahan, I., Ceribasi, A.O., Karaoglu, A., et al., 2005. Effects of lycopene against cisplatin-induced nephrotoxicity and oxidative stress in rats. *Toxicology* 212 (2–3), 116–123. <https://doi.org/10.1016/j.tox.2005.04.016>.
- Avalos-Soriano, A., De la Cruz-Cordero, R., Rosado, J.L., Garcia-Gasca, T., 2016. 4-Hydroxyisoleucine from fenugreek (*Trigonella foenum-graecum*): effects on insulin resistance associated with obesity. *Molecules* 21 (11), 1596. <https://doi.org/10.3390/molecules21111596>.
- Bayrak, O., Bavbek, N., Karatas, O.F., Bayrak, R., Catal, F., Cimentepe, E., et al., 2008. *Nigella sativa* protects against ischaemia/reperfusion injury in rat kidneys. *Nephrol. Dial. Transplant.* 23 (7), 2206–2212. <https://doi.org/10.1093/ndt/gfm953>.
- Bencheikh, N., Bouhrim, M., Kharhoufa, L., Al Kamaly, O.M., Mechchate, H., Es-Safi, I., et al., 2021. The nephroprotective effect of *Zizyphus lotus* L. (Desf.) fruits in a gentamicin-induced acute kidney injury model in rats: a biochemical and histopathological investigation. *Molecules* 26 (16), 4806. <https://doi.org/10.3390/molecules26164806>.
- Bilgiç, S., Korkmaz, D.T., Azirak, S., Güvenç, A.N., Kocaman, N., Özer, M.K., 2017. Risperidone-induced renal damage and metabolic side effects: the protective effect of resveratrol. *Oxid. Med. Cell. Longev.* 2017, 8709521. <https://doi.org/10.1155/2017/8709521>.
- Bopana, N., Saxena, S., 2007. *Asparagus racemosus*—ethnopharmacological evaluation and conservation needs. *J. Ethnopharmacol.* 110 (1), 1–15. <https://doi.org/10.1016/j.jep.2007.01.001>.
- Cao, Y.L., Lin, J.H., Hammes, H.P., Zhang, C., 2022. Flavonoids in treatment of chronic kidney disease. *Molecules* 27 (7), 2365. <https://doi.org/10.3390/molecules27072365>.
- Chakrabarti, S., Jana, M., Roy, A., Pahan, K., 2018. Upregulation of suppressor of cytokine signaling 3 in microglia by cinnamic acid. *Curr. Alzheimer Res.* 15 (10), 894–904. <https://doi.org/10.2174/1567205015666180507104755>.
- Chakraborty, S., Kaur, S., Guha, S., Batra, S.K., 2012. The multifaceted roles of neutrophil gelatinase associated lipocalin (NGAL) in inflammation and cancer. *Biochim. Biophys. Acta* 1826 (1), 129–169. <https://doi.org/10.1016/j.bbcan.2012.03.008>.
- Chipuk, J.E., Moldoveanu, T., Llambi, F., Parsons, M.J., Green, D.R., 2010. The BCL-2 family reunion. *Mol. Cell.* 37 (3), 299–310. <https://doi.org/10.1016/j.molcel.2010.01.025>.
- do Nascimento, C.M., Cassol, T., da Silva, F.S., Bonfleur, M.L., Nassar, C.A., Nassar, P.O., 2013. Radiographic evaluation of the effect of obesity on alveolar bone in rats with ligature-induced periodontal disease. *Diabetes Metab. Syndr. Obes.* 6, 365–370. <https://doi.org/10.2147/DMSO.S50105>.
- Elsherbiny, N.M., Al-Gayyar, M.M., 2016. The role of IL-18 in type 1 diabetic nephropathy: the problem and future treatment. *Cytokine* 81, 15–22. <https://doi.org/10.1016/j.cyto.2016.01.014>.
- Fu, Y.S., Chen, T.H., Weng, L., Huang, L., Lai, D., Weng, C.F., 2021. Pharmacological properties and underlying mechanisms of curcumin and prospects in medicinal potential. *Biomed. Pharmacother.* 141, 111888. <https://doi.org/10.1016/j.biopha.2021.111888>.
- Garde, G.K., 1970. Sarth vagbhat (Marathia translation of Vagbhat's Astangahrdaya). *Uttarstana, Aryabhushana Mudranalaya* 40–48.
- Ghasemi, M., Turnbull, T., Sebastian, S., Kempson, I., 2021. The MTT assay: utility, limitations, pitfalls, and interpretation in bulk and single-cell analysis. *Int. J. Mol. Sci.* 22 (23), 12827. <https://doi.org/10.3390/ijms222312827>.
- Guo, C., Yuan, H., He, Z., 2012. Melamine causes apoptosis of rat kidney epithelial cell line (NRK-52e cells) via excessive intracellular ROS (reactive oxygen species) and the activation of p38 MAPK pathway. *Cell Biol. Int.* 36 (4), 383–389. <https://doi.org/10.1042/CBI20110504>.
- Han, W.K., Wagener, G., Zhu, Y., Wang, S., Lee, H.T., 2009. Urinary biomarkers in the early detection of acute kidney injury after cardiac surgery. *Clin. J. Am. Soc. Nephrol.* 4 (5), 873–882. <https://doi.org/10.2215/CJN.04810908>.
- Hao, Q., Xiao, X., Zhen, J., Feng, J., Song, C., Jiang, B., et al., 2016. Resveratrol attenuates acute kidney injury by inhibiting death receptor-mediated apoptotic pathways in a cisplatin-induced rat model. *Mol. Med. Rep.* 14 (4), 3683–3689. <https://doi.org/10.3892/mmr.2016.5714>.
- Hassan, S.M., Khalaf, M.M., Sadek, S.A., Abo-Youssef, A.M., 2017. Protective effects of apigenin and myricetin against cisplatin-induced nephrotoxicity in mice. *Pharmacut. Biol.* 55 (1), 766–774. <https://doi.org/10.1080/13880209.2016.1275704>.
- Hassanein, E.H.M., Shalkami, A.S., Khalaf, M.M., Mohamed, W.R., Hemeida, R.A.M., 2019. The impact of Keap1/Nrf2, P38MAPK/NF- κ B and Bax/Bcl2/caspase-3 signaling pathways in the protective effects of berberine against methotrexate-induced nephrotoxicity. *Biomed. Pharmacother.* 109, 47–56. <https://doi.org/10.1016/j.biopha.2018.10.088>.
- Hauner, H., Hastreiter, L., Werdier, D., Chen-Stute, A., Scholze, J., Blüher, M., 2017. Efficacy and safety of cathine (Nor-Pseudoephedrine) in the treatment of obesity: a randomized dose-finding study. *Obes. Facts* 10 (4), 407–419. <https://doi.org/10.1159/000478098>.
- He, X., Wen, Y., Wang, Q., Wang, Y., Zhang, G., Wu, J., et al., 2021. Apigenin nanoparticle attenuates renal ischemia/reperfusion inflammatory injury by regulation of miR-140-5p/CXCL12/NF- κ B signaling pathway. *J. Biomed. Nanotechnol.* 17 (1), 64–77. <https://doi.org/10.1166/jbn.2021.3010>.
- Hussein, M.M., Althagafi, H.A., Alharthi, F., Albrakati, A., Alsharif, K.F., Theyab, A., 2022. Apigenin attenuates molecular, biochemical, and histopathological changes associated with renal impairments induced by gentamicin exposure in rats. *Environ. Sci. Pollut. Res. Int.* 29 (43), 65276–65288. <https://doi.org/10.1007/s11356-022-20235-9>.
- Jana, S., Mitra, P., Dutta, A., Khatun, A., Kumar Das, T., Pradhan, S., et al., 2023. Early diagnostic biomarkers for acute kidney injury using cisplatin-induced nephrotoxicity in rat model. *Curr. Res. Toxicol.* 5, 100135. <https://doi.org/10.1016/j.crtx.2023.100135>.
- Jana, S., Mitra, P., Roy, S., 2022. Proficient novel biomarkers guide early detection of acute kidney injury: a review. *Diseases* 11 (1), 8. <https://doi.org/10.3390/diseases11010008>.
- Jiang, N., Doseff, A.L., Grotewold, E., 2016. Flavones: from biosynthesis to health benefits. *Plants* 5 (2), 27. <https://doi.org/10.3390/plants5020027>.
- Kalluri, R., Weinberg, R.A., 2009. The basics of epithelial-mesenchymal transition. *J. Clin. Invest.* 119 (6), 1420–1428. <https://doi.org/10.1172/JCI39104>.
- Kamat, J.P., Boloor, K.K., Devasagayam, T.P., Venkatachalam, S.R., 2000. Antioxidant properties of *Asparagus racemosus* against damage induced by gamma-radiation in rat liver mitochondria. *J. Ethnopharmacol.* 71 (3), 425–435. [https://doi.org/10.1016/S0378-8741\(00\)00176-8](https://doi.org/10.1016/S0378-8741(00)00176-8).
- Kara, Ö., Kilitci, A., Dağlıoğlu, G., 2022. Protective effect of resveratrol on cisplatin induced damage in rat kidney. *Cukurova Med. J.* 47 (3), 990–995.
- Kasali, F.M., Kadima, J.N., Tusiimire, J., Ajayi, C.O., Agaba, A.G., 2022. Effects of the oral administration of aqueous and methanolic leaf extracts of *Chenopodium ambrosioides* L. (Amaranthaceae) on blood Glucose levels in wistar rats. *J. Exp. Pharmacol.* 14, 139–148. <https://doi.org/10.2147/JEP.S356564>.
- Khairam, S.I., Kulkarni, Y.A., Singh, K., 2024. Mitigation of cisplatin-induced nephrotoxicity by chelidonic acid in Wistar rats. *J. Trace. Elem. Med. Biol.* 81, 127321. <https://doi.org/10.1016/j.jtemb.2023.127321>.
- Kitada, M., Koya, D., 2013. Renal protective effects of resveratrol. *Oxid. Med. Cell. Longev.* 2013, 568093. <https://doi.org/10.1155/2013/568093>.
- Kong, W.J., Vernieri, C., Foiani, M., Jiang, J.D., 2020. Berberine in the treatment of metabolism-related chronic diseases: a drug cloud (dCloud) effect to target multifactorial disorders. *Pharmacol. Ther.* 209, 107496. <https://doi.org/10.1016/j.pharmthera.2020.107496>.
- Korrapati, M.C., Shaner, B.E., Schnellmann, R.G., 2012. Recovery from glycerol-induced acute kidney injury is accelerated by suramin. *J. Pharmacol. Exp. Therapeut.* 341 (1), 126–136. <https://doi.org/10.1124/jpet.111.190249>.
- Kumar, D., Singla, S.K., Puri, V., Puri, S., 2015. The restrained expression of NF- κ B in renal tissue ameliorates folic acid induced acute kidney injury in mice. *PLoS One* 10 (1), e115947. <https://doi.org/10.1371/journal.pone.0115947>.
- Lam, K.Y., Ling, A.P., Koh, R.Y., Wong, Y.P., Say, Y.H., 2016. A review on medicinal properties of orientin. *Adv. Pharmacol. Sci.* 2016, 4104595. <https://doi.org/10.1155/2016/4104595>.
- Lateef, R., Mandal, P., Ansari, K.M., Akhtar, M.J., Ahamed, M., 2023. Cytotoxicity and apoptosis induction of copper oxide-reduced graphene oxide nanocomposites in normal rat kidney cells. *J. King Saud Univ. Sci.* 35 (2), 102513.
- Li, B., Jiang, T., Liu, H., Miao, Z., Fang, D., Zheng, L., et al., 2018. Andrographolide protects chondrocytes from oxidative stress injury by activation of the Keap1-Nrf2-Are signaling pathway. *J. Cell. Physiol.* 234 (1), 561–571. <https://doi.org/10.1002/jcp.26769>.
- Lin, M.T., Ko, J.L., Liu, T.C., Chao, P.T., Ou, C.C., 2018. Protective effect of D-methionine on body weight loss, anorexia, and nephrotoxicity in cisplatin-induced chronic

- toxicity in rats. *Integr. Cancer Ther.* 17 (3), 813–824. <https://doi.org/10.1177/1534735417753543>.
- Lin, Y.C., Hwu, Y., Huang, G.S., Hsiao, M., Lee, T.T., Yang, S.M., et al., 2017. Differential synchrotron X-ray imaging markers based on the renal microvasculature for tubulointerstitial lesions and glomerulopathy. *Sci. Rep.* 7 (1), 3488. <https://doi.org/10.1038/s41598-017-03677-x>.
- Liu, M., Grigoryev, D.N., Crow, M.T., Haas, M., Yamamoto, M., Reddy, S.P., et al., 2009. Transcription factor Nrf2 is protective during ischemic and nephrotoxic acute kidney injury in mice. *Kidney Int.* 76 (3), 277–285. <https://doi.org/10.1038/ki.2009.157>.
- Livak, K.J., Schmittgen, T.D., 2001. Analysis of relative gene expression data using real-time quantitative PCR and the 2(-Delta Delta C(T)) Method. *Methods* 25 (4), 402–408. <https://doi.org/10.1006/meth.2001.1262>.
- Ma, N., Wei, W., Fan, X., Ci, X., 2019. Farnesol attenuates cisplatin-induced nephrotoxicity by inhibiting the reactive oxygen species-mediated oxidation, inflammation, and apoptotic signaling pathways. *Front. Physiol.* 10, 1419. <https://doi.org/10.3389/fphys.2019.01419>.
- Macedo, E., Wiggers, H.J., Silva, M.G., Braz-Filho, R., Andricopulo, A.D., Montanari, C. A., 2009. A new bianthron glycoside as inhibitor of *Trypanosoma cruzi* glyceraldehyde 3-phosphate dehydrogenase activity. *J. Brazilian Chem. Soc.* 20, 947–953. <https://doi.org/10.1590/S0103-50532009000500021>.
- Mandal, S.C., Nandy, A., Pal, M., Saha, B.P., 2000. Evaluation of antibacterial activity of *Asparagus racemosus* willd. root. *Phytother. Res.* PTR 14 (2), 118–119. [https://doi.org/10.1002/\(sici\)1099-1573\(200003\)14:2<118::aid-ptr493>3.0.co;2-p](https://doi.org/10.1002/(sici)1099-1573(200003)14:2<118::aid-ptr493>3.0.co;2-p).
- McSweeney, K.R., Gadanec, L.K., Qaradahi, T., Ali, B.A., Zulli, A., Apostolopoulos, V., 2021. Mechanisms of cisplatin-induced acute kidney injury: pathological mechanisms, pharmacological interventions, and genetic mitigations. *Cancers* 13 (7), 1572. <https://doi.org/10.3390/cancers13071572>.
- Meghji, K.A., Talpur, R.A., Uqaili, A.A., Nizammani, Y.M., Kazi, N., Nizammani, G.S., 2019. Resveratrol attenuates oxidative stress in chemotherapy induced acute kidney injury: an experimental rat model. *Khyber Med. Univ. J.* 11 (2), 85–89.
- Meka Kadir, W., Dukassa Dubiwak, A., Tofik Ahmed, E., 2022. Nephroprotective effect of *Asparagus africanus* lam. Root extract against gentamicin-induced nephrotoxicity in Swiss albino mice. *J. Toxicol.* 2022, 8440019. <https://doi.org/10.1155/2022/8440019>.
- Meng, X.M., Li, H.D., Wu, W.F., Ming-Kuen Tang, P., Ren, G.L., Gao, L., et al., 2018. Wogonin protects against cisplatin-induced acute kidney injury by targeting RIPK1-mediated necroptosis. *Lab. Invest.* 98 (1), 79–94. <https://doi.org/10.1038/labinvest.2017.115>.
- Mihanfar, A., Darband, S.G., Sadighparvar, S., Kaviani, M., Mirza-Aghazadeh-Attari, M., Yousefi, B., et al., 2021. *In vitro* and *in vivo* anticancer effects of syringic acid on colorectal cancer: possible mechanistic view. *Chem. Biol. Interact.* 337, 109337. <https://doi.org/10.1016/j.cbi.2020.109337>.
- Mitra, P., Jana, S., Roy, S., 2024. Insights into the therapeutic uses of plant derive phytochemicals on diabetic nephropathy. *Curr. Diabetes Rev.* 20 (9), 62–76. <https://doi.org/10.2174/0115733998273395231117114600>.
- Mitra, S.K., Prakash, N.S., Sundaram, R., 2012. Shatavarins (containing Shatavarin IV) with anticancer activity from the roots of *Asparagus racemosus*. *Indian J. Pharmacol.* 44 (6), 732–736. <https://doi.org/10.4103/0253-7613.103273>.
- Molaei, E., Molaei, A., Abedi, F., Hayes, A.W., Karimi, G., 2021. Nephroprotective activity of natural products against chemical toxicants: the role of Nrf2/ARE signaling pathway. *Food Sci. Nutr.* 9 (6), 3362–3384. <https://doi.org/10.1002/fsn3.2320>.
- Mushtaq, Z., Sadeer, N.B., Hussain, M., Mahwish, Alsagaby, S.A., Imran, M., Mumtaz, T., et al., 2023. Therapeutical properties of apigenin: a review on the experimental evidence and basic mechanisms. *Int. J. Food Prop.* 26 (1), 1914–1939. <https://doi.org/10.1080/10942912.2023.2236329>.
- Naruta, E., Buko, V., 2001. Hypolipidemic effect of pantothenic acid derivatives in mice with hypothalamic obesity induced by aurothioglucose. *Exp. Toxicol. Pathol.* 53 (5), 393–398. <https://doi.org/10.1078/0940-2993-00205>.
- Niture, S.K., Jaiswal, A.K., 2012. Nrf2 protein up-regulates antiapoptotic protein Bcl-2 and prevents cellular apoptosis. *J. Biol. Chem.* 287 (13), 9873–9886. <https://doi.org/10.1074/jbc.M111.312694>.
- OECD, 2002. Test No. 423: acute oral toxicity-acute toxic class method. *OECD Guidel. Test. Chem.* 4, 14. Section.
- Ognjanović, B.I., Djordjević, N.Z., Matic, M.M., Obradović, J.M., Mladenović, J.M., Stajin, A.S., et al., 2012. Lipid peroxidative damage on Cisplatin exposure and alterations in antioxidant defense system in rat kidneys: a possible protective effect of selenium. *Int. J. Mol. Sci.* 13 (2), 1790–1803. <https://doi.org/10.3390/ijms13021790>.
- Ogut, E., Armagan, K., Gül, Z., 2022. The role of syringic acid as a neuroprotective agent for neurodegenerative disorders and future expectations. *Metab. Brain Dis.* 37 (4), 859–880. <https://doi.org/10.1007/s11011-022-00960-3>.
- Oh, G.S., Kim, H.J., Shen, A., Lee, S.B., Khadka, D., Pandit, A., et al., 2014. Cisplatin-induced kidney dysfunction and perspectives on improving treatment strategies. *Electroly. Blood Press* 12 (2), 55–65. <https://doi.org/10.5049/EBP.2014.12.2.55>.
- Ortega-Domínguez, B., Aparicio-Trejo, O.E., García-Arroyo, F.E., León-Contreras, J.C., Tapia, E., Molina-Jijón, E., et al., 2017. Curcumin prevents cisplatin-induced renal alterations in mitochondrial bioenergetics and dynamic. *Food Chem. Toxicol.* 107 (Pt A), 373–385. <https://doi.org/10.1016/j.fct.2017.07.018>.
- Osman, A.M., Telity, S.A., Telity, S.A., Damanhour, Z.A., Al-Harthy, S.E., Al-Kreathy, 2015. Chemosensitizing and nephroprotective effect of resveratrol in cisplatin-treated animals. *Cancer Cell Int.* 15, 6. <https://doi.org/10.1186/s12935-014-0152-2>.
- Palatini, P., 2012. Glomerular hyperfiltration: a marker of early renal damage in pre-diabetes and pre-hypertension. *Nephrol. Dial. Transplant.* 27 (5), 1708–1714. <https://doi.org/10.1093/ndt/gfs037>.
- Pham, T.V., Ngo, H.P.T., Nguyen, N.H., Do, A.T., Vu, T.Y., Nguyen, M.H., et al., 2023. The anti-inflammatory activity of the compounds isolated from *Dichroa febrifuga* leaves. *Saudi J. Biol. Sci.* 30 (4), 103606. <https://doi.org/10.1016/j.sjbs.2023.103606>.
- Purena, R., Seth, R., Bhatt, R., 2018. Protective role of *Emblcia officinalis* hydro-ethanolic leaf extract in cisplatin induced nephrotoxicity in Rats. *Toxicol Rep* 5, 270–277. <https://doi.org/10.1016/j.toxrep.2018.01.008>.
- Quan, H., Sun, N., Liu, S., Li, M., Wang, H., Wang, Z., 2021. The analysis of flavonoids and triterpenes extracted from *Urtica* by LC-MS and the antimicrobial activity of the extracts. *J. Food Process. Preserv.* 45 (9), e15706. <https://doi.org/10.1111/jfpp.15706>.
- Rizk, S., Abdel Moneim, A.E., Abdel-Gaber, R.A., Alquraishi, M.I., Santourlidis, S., Dkhal, M.A., 2023. Nephroprotective efficacy of *Echinops spinosus* against a glycerol-induced acute kidney injury model. *ACS Omega* 8 (44), 41865–41875. <https://doi.org/10.1021/acsomega.3c06792>.
- Roy, S., Pradhan, S., Mandal, S., Das, K., Nandi, D.K., 2018. Nephroprotective efficacy of *Asparagus racemosus* root extract on acetaminophen-induced renal injury in rats. *Acta Biol. Szeged.* 62 (1), 17–23. <https://doi.org/10.14232/abs.2018.1.17-23>.
- Rysz, J., Gluba-Brzózka, A., Franczyk, B., Jablonowski, Z., Ciałkowska-Rysz, A., 2017. Novel biomarkers in the diagnosis of chronic kidney disease and the prediction of its outcome. *Int. J. Mol. Sci.* 18 (8), 1702. <https://doi.org/10.3390/ijms18081702>.
- Sahu, B.D., Kalvala, A.K., Koneru, M., Mahesh Kumar, J., Kuncha, M., Rachamalla, S.S., et al., 2014. Ameliorative effect of fisetin on cisplatin-induced nephrotoxicity in rats via modulation of NF- κ B activation and antioxidant defence. *PLoS One* 9 (9), e105070. <https://doi.org/10.1371/journal.pone.0105070>.
- Sammani, M.S., Clavijo, S., Figuerola, A., Cerdà, V., 2021. 3D printed structure coated with C18 particles in an online flow system coupled to HPLC-DAD for the determination of flavonoids in citrus external peel. *Micro. J.* 168, 106421. <https://doi.org/10.1016/j.microc.2021.106421>.
- Satta, S., Mahmud, A.M., Wilkinson, F.L., Yvonne Alexander, M., White, S.J., 2017. The role of Nrf2 in cardiovascular function and disease. *Oxid. Med. Cell. Longev.* 2017, 9237263. <https://doi.org/10.1155/2017/9237263>.
- Schmidt-Ott, K.M., Mori, K., Li, J.Y., Kalandadze, A., Cohen, D.J., Devarajan, P., et al., 2007. Dual action of neutrophil gelatinase-associated lipocalin. *J. Am. Soc. Nephrol.* 18 (2), 407–413. <https://doi.org/10.1681/ASN.2006080882>.
- Shao, Y., Chin, C.K., Ho, C.T., Ma, W., Garrison, S.A., Huang, M.T., 1996. Anti-tumor activity of the crude saponins obtained from asparagus. *Cancer Lett.* 104 (1), 31–36. [https://doi.org/10.1016/0304-3835\(96\)04233-4](https://doi.org/10.1016/0304-3835(96)04233-4).
- Sharma, M., Sharma, A., Kumar, A., 2011. Ethnopharmacological importance of *Asparagus racemosus*: a review. *J. Pharmaceut. Biomed. Sci.* 6 (6).
- Shimoyamada, M., Suzuki, M., Sonta, H., Maruyama, M., Okubo, K., 1990. Antifungal activity of the saponin fraction obtained from *Asparagus officinalis* L. and its active principle. *Agric. Biol. Chem.* 54 (10), 2553–2557.
- Singh, N., Garg, M., Prajapati, P., Singh, P.K., Chopra, R., Kumari, A., et al., 2023. Adaptogenic property of *Asparagus racemosus*: future trends and prospects. *Heliyon* 9 (4), e14932. <https://doi.org/10.1016/j.heliyon.2023.e14932>.
- Stael, S., Miller, L.P., Fernández-Fernández, A.D., Van Breusegem, F., 2022. Detection of damage-activated metacaspase activity by western blot in plants. *Methods Mol. Biol.* 2447, 127–137. https://doi.org/10.1007/978-1-0716-2079-3_11.
- Sun, C.Y., Nie, J., Zheng, Z.L., Zhao, J., Wu, L.M., Zhu, Y., et al., 2019. Renoprotective effect of scutellarin on cisplatin-induced renal injury in mice: impact on inflammation, apoptosis, and autophagy. *Biomed. Pharmacother.* 112, 108647. <https://doi.org/10.1016/j.biopha.2019.108647>.
- Takeda, H., Sadakane, C., Hattori, T., Katsurada, T., Ohkawara, T., Nagai, K., et al., 2008. Rikkunshito, an herbal medicine, suppresses cisplatin-induced anorexia in rats via 5-HT2 receptor antagonism. *Gastroenterology* 134 (7), 2004–2013. <https://doi.org/10.1053/j.gastro.2008.02.078>.
- Thimmulappa, R.K., Lee, H., Rangasamy, T., Reddy, S.P., Yamamoto, M., Kensler, T.W., et al., 2006. Nrf2 is a critical regulator of the innate immune response and survival during experimental sepsis. *J. Clin. Invest.* (4), 984–995. <https://doi.org/10.1172/JCI25790>.
- Udupa, V., Prakash, V., 2018. Gentamicin induced acute renal damage and its evaluation using urinary biomarkers in rats. *Toxicol Rep* 6, 91–99. <https://doi.org/10.1016/j.toxrep.2018.11.015>.
- Venkatesan, N., Thiagarajan, V., Narayanan, S., Arul, A., Raja, S., Vijaya Kumar, S.G., et al., 2005. Anti-diarrhoeal potential of *Asparagus racemosus* wild root extracts in laboratory animals. *J. Pharm. Pharmaceut. Sci.: Publ. Canad. Soc. Pharmaceut. Sci. Soc. Canad. des Sci. Pharmaceut.* 8 (1), 39–46.
- Wang, Y., Fu, J., Zhang, C., Zhao, H., 2016. HPLC-DAD-ESI-MS analysis of flavonoids from leaves of different cultivars of sweet osmanthus. *Molecules* 21 (9), 1224. <https://doi.org/10.3390/molecules21091224>.
- Wang, Z., Sun, W., Sun, X., Wang, Y., Zhou, M., 2020. Kaempferol ameliorates Cisplatin induced nephrotoxicity by modulating oxidative stress, inflammation and apoptosis via ERK and NF- κ B pathways. *Amb. Express* 10 (1), 58. <https://doi.org/10.1186/s13568-020-00993-w>.
- Wu, Q., Li, W., Zhao, J., Sun, W., Yang, Q., Chen, C., 2021. Apigenin ameliorates doxorubicin-induced renal injury via inhibition of oxidative stress and inflammation. *Biomed. Pharmacother. = Biomedicine & pharmacotherapie* 137, 111308. <https://doi.org/10.1016/j.biopha.2021.111308>.
- Xu, M., Li, S., Wang, J., Huang, S., Zhang, A., Zhang, Y., et al., 2021. Cilomilast ameliorates renal tubulointerstitial fibrosis by inhibiting the TGF- β 1-smad2/3 signaling pathway. *Front. Med.* 7, 626140. <https://doi.org/10.3389/fmed.2020.626140>.
- Xue, J.L., Liu, B.Y., Zhao, M., Zhang, M.Y., Wang, M.Y., Gu, Q.Q., et al., 2023. Inhalation of 4% and 67% hydrogen ameliorates oxidative stress, inflammation, apoptosis, and

- necroptosis in a rat model of glycerol-induced acute kidney injury. *Med. Gas Res.* 13 (2), 78–88. <https://doi.org/10.4103/2045-9912.345169>.
- Yang, S., Chou, G., Li, Q., 2018. Cardioprotective role of azafrin in against myocardial injury in rats via activation of the Nrf2-ARE pathway. *Phytomedicine* 47, 12–22. <https://doi.org/10.1016/j.phymed.2018.04.042>.
- Zhang, L.X., Li, C.X., Kakar, M.U., Khan, M.S., Wu, P.F., Amir, R.M., et al., 2021. Resveratrol (RV): a pharmacological review and call for further research. *Biomed. Pharmacother.* 143, 112164. <https://doi.org/10.1016/j.biopha.2021.112164>.
- Zhang, Z., Lu, B., Sheng, X., Jin, N., 2011. Cystatin C in prediction of acute kidney injury: a systemic review and meta-analysis. *Am. J. Kidney Dis.* 58 (3), 356–365. <https://doi.org/10.1053/j.ajkd.2011.02.389>.